A Low ML-decoding Complexity, Full-diversity, Full-rate MIMO Precoder

K. Pavan Srinath and B. Sundar Rajan,

Dept of ECE, Indian Institute of science,

Bangalore 560012, India

Email:{pavan,bsrajan}@ece.iisc.ernet.in

Abstract

Precoding for multiple-input, multiple-output (MIMO) antenna systems is considered with perfect channel knowledge available at both the transmitter and the receiver. For 2 transmit antennas and QAM constellations, an approximately optimal (with respect to the minimum Euclidean distance between points in the received signal space) real-valued precoder based on the singular value decomposition (SVD) of the channel is proposed, and it is shown to offer a maximum-likelihood (ML)-decoding complexity of $\mathcal{O}(\sqrt{M})$ for square M-QAM. The proposed precoder is obtainable easily for arbitrary QAM constellations, unlike the known complex-valued optimal precoder by Collin et al. for 2 transmit antennas, which is in existence for 4-QAM alone with an ML-decoding complexity of $\mathcal{O}(M\sqrt{M})$ ($M = 4$) and is extremely hard to obtain for larger QAM constellations. The proposed precoder's loss in error performance for 4-QAM in comparison with the complex-valued optimal precoder is only marginal. Our precoding scheme is extended to higher number of transmit antennas on the lines of the E-d_{min} precoder for 4-QAM by Vrigneau et al. which is an extension of the complex-valued optimal precoder for 4-QAM. Compared with the recently proposed $X-$ and $Y-$precoders, the error performance of our precoder is significantly better. It is shown that our precoder provides full-diversity for QAM constellations and this is supported by simulation plots of the word error probability for 2×2, 4×4 and 8×8 systems.

Index Terms

Diversity gain, low ML-decoding complexity, MIMO precoders, singular values, word error probability.

I. INTRODUCTION AND BACKGROUND

Multiple-input, multiple-output (MIMO) antenna systems have evoked a lot of research interest primarily because of the enhanced capacity they provide, compared with that provided by the single antenna

point to point channel. Moreover, for a system with n_t transmit antennas and n_r receive antennas ($n_t \times n_r$ system), the maximum *diversity gain* (refer Section II for a definition of diversity gain) achievable with coherent detection has been shown to be $n_t n_r$. For MIMO systems with the channel state information available only at the receiver (CSIR), suitably designed space-time block codes (STBCs) [1] provide full-diversity. Full-rate transmission is said to occur if $n_{min} = \min(n_t, n_r)$ independent information symbols are transmitted in every channel use. Full-rate STBCs achieving full-diversity have also been proposed [2], [3]. However, all full-rate, full-diversity STBCs are characterized by a high ML-decoding complexity (refer Section II for a formal definition of ML-decoding complexity). In general, decoding full-rate STBCs requires jointly decoding $n_t n_{min}$ symbols.

MIMO systems with full channel state information at the transmitter (CSIT) or partial CSIT have been extensively studied in literature. From an information-theoretic perspective, capacity is an important parameter for MIMO systems and waterfilling [4] can be employed to achieve the capacity with a Gaussian codebook. From a signal processing point of view, the error performance of MIMO systems using finite constellations is one of the important parameters, and several precoding[1] schemes have been proposed in this regard. Maximal ratio transmission was introduced in [5] to achieve full-diversity while maximizing the signal-to-noise ratio (SNR) by precoding at the transmitter and equalizing at the receiver for transmission of a single symbol per channel use. Subsequently, the use of precoding and equalizing matrices at the transmitter and the receiver, respectively, was proposed in [6] to maximize the SNR at the receiver, but this scheme resulted in low-rate transmission. Several works on optimal linear precoders and decoders have been done for the *minimum mean square error* (MMSE) criterion [7]-[10]. Since these precoders are linear and optimal for the MMSE decoding, the decoding complexity is very low and full-diversity is also achieved, but the error performance is worse than that for the ML-decoding. Other non-ML-decoding techniques include lattice-reduction based techniques [11] which provide full-rate transmission with possibly full-diversity, but lattice-reduction itself involves a high complexity for large MIMO systems. Extensive research has also been done on MIMO systems with limited feedback to the transmitter about the channel from the receiver (see, for example, [12] and references therein). In this paper, we consider MIMO systems with full CSIT. The channel state information could be either sent to the transmitter by the receiver (when there are separate frequency bands for uplink and downlink transmission) or the transmitter could estimate the channel, if it is reciprocal (like in a time division duplexing (TDD) system), by receiving pilot signals from the receiver. In literature, to the best of our

---

[1]precoding is also referred to as "transmit beamforming".

knowledge, there is no known precoding technique to achieve all the three attributes - full-rate, full-diversity and low ML-decoding complexity ("low ML-decoding complexity" is a relative term and in this paper, it is used to mean the joint decoding of at most 2 complex symbols).

Almost all the popular precoding techniques with ML-decoding at the receiver use the singular value decomposition (SVD) of the MIMO channel [13]. The E-d_{min} precoder for 4-QAM [14], an extension of the complex-valued optimal[2] precoder [15] to higher number of transmit antennas, has been shown to perform very well for 4-QAM, beating all other linear precoding and decoding schemes based on the MMSE criterion, and ML-decoding involves jointly decoding two complex symbols only. However, this precoder exists in literature for 4-QAM alone and is very hard to obtain for larger QAM constellations, since it involves a numerical search over 3 parameters. Recently, X- and Y- precoders have been proposed in [16] as rivals for the E-d_{min} precoder. The X-precoder has been shown to offer an ML-decoding complexity of $\mathcal{O}(M)$ (this can be brought down to $\mathcal{O}(\sqrt{M})$ by the same decoding scheme as for our precoder, which is explained in Subsection IV-D), while the Y-precoder has an ML-decoding complexity which is invariant with respect to the constellation size M. The disadvantage with the X-precoder is that it loses out to the E-d_{min} precoder in error performance for 4-QAM and it is not known if an explicit expression for the precoding matrix can be obtained for larger QAM constellations. The Y-precoder (which uses a two-dimensional constellation), although explicitly obtainable for constellations of any size M, loses out in error performance to the E-d_{min} precoder, since it has not been optimized for error performance. In literature, all the aforementioned low ML-decoding complexity precoders have been claimed to offer a diversity gain of $(n_t - n_{min}/2 + 1)(n_r - n_{min}/2 + 1)$ by the authors (but the simulation results in this paper indicate that the E-d_{min} precoder has full-diversity for 4-QAM). Concerned by the limitations of each of the low ML-decoding complexity precoders, we first propose a real-valued, approximately optimal precoder (we explain in Section IV why the precoder is "approximately optimal") based on the SVD of the channel for $n_t = 2$ and then extend it to higher number of transmit antennas, an approach similar to that in [14]. The ML-decoding complexity offered by our precoder is shown to be $\mathcal{O}(\sqrt{M})$ for M-QAM. For 4-QAM, the proposed precoder has only a marginally poorer error performance than the E-d_{min} precoder, but has lower ML-decoding complexity. For larger QAM constellations, it is easily obtainable, unlike the E-d_{min} precoder. When compared with the X- and Y-precoders, it has a much better error performance. The main contributions of the paper are -

---

[2]Throughout this paper, unless otherwise stated, optimalily is with respect to the minimum Euclidean distance between points in the received signal space.

1) we propose a novel scheme to obtain an SVD-based, real-valued, approximately optimal precoder for 2 transmit antennas and any M-QAM. The method of obtaining this precoder is different from the one taken to obtain the complex-valued optimal precoder for 2 transmit antennas [15], and is easily applicable for any M-QAM, unlike that in [15].

2) We extend this real-valued precoder to higher number of transmit antennas and show that our precoding scheme offers full-diversity with ML-decoding. This is a new result as the existing low ML-decoding complexity precoders have been claimed to offer a diversity gain of only $(n_t - n_{min}/2 + 1)(n_r - n_{min}/2 + 1)$. The simulation plots of the word error probability for 2×2, 4×4 and 8×8 systems support our claims about full-diversity.

3) The ML-decoding complexity of the proposed precoder is shown to be $\mathcal{O}(\sqrt{M})$ for square M-QAM, in general. However, for a considerable number of channel realizations, no search is required over the M signal points. Specifically for 4-QAM and 2 transmit antennas, simulations reveal that for more than 50% of the channel realizations, no search is needed over any of the signal points. This aspect is elaborated in Subsection IV-D.

The rest of the paper is organized as follows. Section II gives the system model, the relevant definitions and some known results which are needed for our precoder design. A brief review of existing low ML-decoding complexity precoders is given in Section III The method to obtain the proposed precoder is presented in Section IV and its ML-decoding complexity is analyzed in Subsection IV-D. In Section V, we show how this precoding scheme can be extended to higher number of transmit antennas while Section VI deals with the achievable diversity gain with the proposed precoder. Simulation results are given in Secion VII and concluding remarks constitute Section VIII.

Notations: Throughout, bold, lowercase letters are used to denote vectors and bold, uppercase letters are used to denote matrices. For a complex matrix $\mathbf{X}$, the Hermitian, the transpose and the Frobenius norm of $\mathbf{X}$ are denoted by $\mathbf{X}^H$, $\mathbf{X}^T$ and $\|\mathbf{X}\|$, respectively. The ith element of a vector $\mathbf{x}$ is denoted by $[\mathbf{x}]_i$, the $(i,j)^{th}$ entry of $\mathbf{X}$ is denoted by $\mathbf{X}(i,j)$, $tr(\mathbf{X})$ denotes the trace of $\mathbf{X}$, and $\mathbf{X} = \text{diag}(x_1, x_2, \cdots, x_n)$ implies that $\mathbf{X}$ is a diagonal matrix with $x_1, x_2, \cdots, x_n$ as the diagonal entries. The set of all real numbers, complex numbers and integers are denoted by $\mathbb{R}$, $\mathbb{C}$ and $\mathbb{Z}$, respectively. The real and the imaginary part of a complex-valued vector $\mathbf{x}$ are denoted by $\mathbf{x}_I$ and $\mathbf{x}_Q$, respectively, $|x|$ denotes the absolute value of a complex number x and $|\mathcal{S}|$ denotes the cardinality of the set $\mathcal{S}$. The $T \times T$ identity matrix and the $n \times m$ sized null matrix are denoted by $\mathbf{I}_T$ and $\mathbf{O}_{n \times m}$, respectively. For a complex random variable X, $\mathbb{E}[X]$ denotes the expectation of X, while $X \sim \mathcal{N}_{\mathbb{C}}(0,1)$ implies that X has the complex normal distribution

with zero mean and unit variance. Unless used as a subscript or to denote indices, j represents $\sqrt{-1}$ and for a function $f(x)$, $\operatorname*{argmin}_x f(x)$ and $\operatorname*{argmax}_x f(x)$ denote that value of x which minimizes and maximizes $f(x)$, respectively. For any real number m, $\lfloor m \rfloor$ denotes the largest integer smaller than m, $\lceil m \rceil$ denotes the smallest integer larger than m, $\operatorname{rnd}[m]$ denotes the operation that rounds off m to the nearest integer and $\operatorname{sgn}(m)$ gives the sign of m, both of which can be expressed as

$$\operatorname{rnd}[m] = \begin{cases} \lfloor m \rfloor, & \text{if } \lceil m \rceil - m > m - \lfloor m \rfloor \\ \lceil m \rceil, & \text{otherwise} \end{cases}, \qquad \operatorname{sgn}(m) = \begin{cases} 1, & \text{if } m \geq 0 \\ -1, & \text{otherwise}. \end{cases}$$

The Gamma function and the Q-function of x are denoted by $\Gamma(x)$ and $Q(x)$, respectively, and given as

$$\Gamma(x) = \int_0^\infty e^{-t} t^{x-1} dt, \qquad Q(x) = \int_x^\infty \frac{1}{\sqrt{2\pi}} e^{-\frac{t^2}{2}} dt.$$

Let $f(x)$ and $g(x)$ be two functions. Then, $f(x) = \mathcal{O}(g(x))$ if and only if there exists a positive constant $c < \infty$ such that

$$\lim_{x \to \infty} \frac{f(x)}{g(x)} = c,$$

and $f(x) = o(g(x))$ as $x \to a$ if and only if

$$\lim_{x \to a} \frac{f(x)}{g(x)} = 0.$$

For a real variable t, the unit step function $u(t)$ is defined as $u(t) = 1$, if $t > 0$, and $u(t) = 0$, if $t < 0$.

II. SYSTEM MODEL

We consider an $n_t \times n_r$ MIMO system with full CSIT and CSIR. The channel is assumed to be quasi-static and flat with Rayleigh fading. The channel is modelled as

$$\mathbf{y} = \sqrt{\frac{SNR}{n_t}} \mathbf{H} \mathbf{s} + \mathbf{n}, \tag{1}$$

where $\mathbf{y} \in \mathbb{C}^{n_r \times 1}$ is the received vector, $\mathbf{H} \in \mathbb{C}^{n_r \times n_t}$ is the channel matrix, $\mathbf{s} \in \mathbb{C}^{n_t \times 1}$ is the precoded symbol vector and $\mathbf{n} \in \mathbb{C}^{n_r \times 1}$ is the noise vector. The entries of $\mathbf{H}$ and $\mathbf{n}$ are i.i.d. circularly symmetric complex Gaussian random variables with zero mean and variance 0.5 per real dimension. In (1), the scalar SNR is the average SNR at each receive antenna, and $\mathbf{s}$ is constrained such that $\mathbb{E}[tr(\mathbf{s}\mathbf{s}^H)] = n_t$. The precoded symbol vector $\mathbf{s}$ can be defined as

$$\mathbf{s} \triangleq \frac{1}{\sqrt{E}} \mathbf{M} \mathbf{x},$$

where $\mathbf{M} \in \mathbb{C}^{n_t \times n_{min}}$ is the precoding matrix, with $\|\mathbf{M}\|^2 = n_t$, and $\mathbf{x} \triangleq [x_1, x_2, \cdots, x_{n_{min}}]^T$ is the symbol vector, with its entries taking values independently from a signal constellation denoted by $\mathcal{A}$, having an average energy of E units. The rate of transmission is n_{min} independent symbols per channel use. Note that in this model, the variable scalar which defines the average SNR at each receive antenna is SNR, while E is a constant. For example, for a standard M-QAM, with $M = 2^{2a}$ for some positive integer a, $E = 2(M-1)/3$.

Let $\mathbf{H} = \mathbf{UDV}^H$, obtained on the SVD of $\mathbf{H}$, with $\mathbf{U} \in \mathbb{C}^{n_r \times n_r}$ and $\mathbf{V} \in \mathbb{C}^{n_t \times n_t}$ being unitary matrices. $\mathbf{D} \in \mathbb{R}^{n_r \times n_t}$ is such that $\mathbf{D} = [\mathbf{D}_1 \quad \mathbf{O}_{n_r \times (n_t - n_r)}]$ if $n_t \geq n_r$ and $\mathbf{D} = [\mathbf{D}_1 \quad \mathbf{O}_{n_t \times (n_r - n_t)}]^T$ if $n_t < n_r$, where $\mathbf{D}_1 \in \mathbb{R}^{n_{min} \times n_{min}}$ is a diagonal matrix given by $\mathbf{D}_1 = \mathrm{diag}(\sigma_1, \sigma_2, \cdots, \sigma_{n_{min}})$, with $\sigma_1, \sigma_2, \cdots, \sigma_{n_{min}}$ being the non-zero singular values of $\mathbf{H}$, placed in the descending order on the diagonal. Let the precoding matrix $\mathbf{M}$ be given as

$$\mathbf{M} = \mathbf{VP}, \tag{2}$$

where $\mathbf{P} \in \mathbb{C}^{n_t \times n_{min}}$. Now, (1) can be written as

$$\mathbf{y}' = \sqrt{\frac{SNR}{n_t E}} \mathbf{DPx} + \mathbf{n}', \tag{3}$$

where $\mathbf{y}' = \mathbf{U}^H \mathbf{y}$ and $\mathbf{n}' = \mathbf{U}^H \mathbf{n}$, with the distribution of $\mathbf{n}'$ being the same as that of $\mathbf{n}$.

The ML-decoding rule seeks to find that $\check{\mathbf{x}} \in \mathcal{A}^{n_{min} \times 1}$ which minimizes the metric given by

$$m(\mathbf{x}) = \left\| \mathbf{y}' - \sqrt{\frac{SNR}{n_t E}} \mathbf{DPx} \right\|^2. \tag{4}$$

Clearly, the error performance of the system depends on the choice of $\mathbf{P}$ and $\mathcal{A}$. From (2), it is evident that the design of the precoding matrix $\mathbf{M}$ amounts to designing $\mathbf{P}$. Henceforth in this paper, $\mathbf{P}$ is referred to as *precoder* and the constellation is assumed to be an M-QAM, where $M = 2^{2a}$ for some positive integer a.

Definition 1: (*Full-diversity precoder*) In a MIMO system, if at a high SNR, the average probability P_e that a transmitted symbol vector is wrongly decoded is given by

$$P_e \approx (G_c.SNR)^{-G_d},$$

where $\approx$ stands for "is approximately equal to", then, G_d and G_c are called the *diversity gain* (or diversity order) and the *coding gain* of the system, respectively. For a MIMO system with precoding, if $G_d = n_t n_r$, then, we call the precoder a full-diversity precoder.

Definition 2: (*ML-Decoding complexity*) The ML decoding complexity is measured in terms of the number of computations involved in minimizing the ML-decoding metric given in (4) and is a function of the constellation size M. If at most k symbols are required to be jointly decoded, the ML-decoding complexity is said to be $\mathcal{O}(M^k)$.

Note that the above definition of the ML-decoding complexity is with respect to the *worst-case* ML-decoding complexity. The use of a sphere decoder [17] can effectively result in a much lower *average* ML-decoding complexity that depends on the dimension of the sphere decoder and not on the constellation size [18]. For a complex lattice constellation of size M, if the ML-decoding complexity is $\mathcal{O}\left(M^k\right)$, the dimension of the real-valued sphere decoder to be used would be $2k$. As a result, a precoding scheme with higher worst-case ML-decoding complexity than another precoding scheme will also have higher average ML-decoding complexity. Hence, throughout this paper, we consider only the worst case ML-decoding complexity.

We make use of the following known results, which are needed for our purpose.

Theorem 1: [19] For a scalar channel modelled by $y = \sqrt{SNR}\beta x + n$, where $n \sim \mathcal{N}_{\mathbb{C}}\left(0,1\right)$, $\mathbb{E}[|x|^2] = 1$ and $\alpha = |\beta|^2$ is a nonnegative random variable whose probability density function (PDF) $f_\alpha(\alpha)$ is such that

$$f_\alpha(\alpha) = c\alpha^t + o(\alpha^t), \quad \text{as } \alpha \to 0^+,$$

the average symbol error probability (SEP) P_e, which is given by

$$P_e = \mathbb{E}[P_{e,\alpha}] = \int_0^\infty Q\left(\sqrt{k\alpha SNR}\right) f_\alpha d\alpha,$$

is such that as $SNR \to \infty$,

$$P_e = \frac{2^t c\Gamma(t+\frac{3}{2})}{\sqrt{\pi}(t+1)}(k.SNR)^{-(t+1)} + o\left(SNR^{-(t+1)}\right),$$

where k is a fixed positive constant depending on the constellation, c is another constant defining the marginal PDF of α and $P_{e,\alpha} = Q\left(\sqrt{k\alpha SNR}\right)$ is the α dependent instantaneous SEP. If $\mathbb{E}[\alpha] = 1$, then, SNR is the average SNR at the receiver and the diversity gain G_d and the coding gain G_c can be defined as

$$G_d = t+1, \quad G_c = k\left(\frac{2^t c\Gamma(t+\frac{3}{2})}{\sqrt{\pi}(t+1)}\right)^{-\frac{1}{t+1}}.$$

Given that σ_i, $i = 1, 2, \cdots, n_{min}$, are the non-zero singular values of $\mathbf{H}$, it is known that σ_i^2 are the non-zero eigenvalues of $\mathbf{H}\mathbf{H}^H$, which are denoted in the descending order by λ_i, $i = 1, 2, \cdots, n_{min}$.

The following theorem gives the expression for the first order expansion of the marginal PDF of λ_i as $\lambda_i \to 0^+$.

Theorem 2: [20] Let the entries of the $n_r \times n_t$ matrix $\mathbf{H}$ be i.i.d. complex Gaussian with zero mean and unit variance. The first order expansion of the marginal PDF of the kth largest eigenvalue λ_k of the complex central Wishart matrix $\mathbf{H}\mathbf{H}^H$ is given by $f_{\lambda_k}(\lambda_k) = a_k \lambda_k^{d_k} + o\left(\lambda_k^{d_k}\right)$, as $\lambda_k \to 0^+$, $k = 1, 2, \cdots, n_{min}$, with $d_k = (n_t - k + 1)(n_r - k + 1) - 1$ and a_k being positive constants.

In (3), if $\mathbf{P} = \mathbf{I}_{n_t}$ or $\mathbf{P} = [\mathbf{I}_{n_r} \quad \mathbf{O}_{n_r \times n_t - n_r}]^T$, depending on whether $n_{min} = n_t$ or $n_{min} = n_r$, respectively, each of the symbols x_i, $i = 1, 2, \cdots, n_{min}$ will experience a diversity gain given by $G_{d_i} = (n_t - i + 1)(n_r - i + 1)$. This is evident from Theorem 1 and Theorem 2. The above operation of premultiplying the symbol vector by $\mathbf{VP}$, with $\mathbf{P} = \mathbf{I}_{n_t}$ (for $n_t < n_r$) or $\mathbf{P} = [\mathbf{I}_{n_r} \quad \mathbf{O}_{n_r \times n_t - n_r}]^T$ (for $n_t \geq n_r$) can be viewed to result in n_{min} *virtual subchannels*. So, the overall diversity gain for the symbol vector is $\min\{G_{d_i}, i = 1, 2, \cdots, n_{min}\} = (n_{max} - n_{min} + 1)$, where $n_{max} = \max(n_t, n_r)$. This is the least diversity order one can obtain in a precoded MIMO system with ML-decoding. However, assuming that the symbols take values from an arbitrary signal constellation of size M, the ML-decoding complexity is $\mathcal{O}(M)$, since each symbol can be decoded independently from the others.

Let $\Delta \mathbf{x} \triangleq \mathbf{x} - \mathbf{x}'$, where $\mathbf{x}, \mathbf{x}' \in \mathcal{A}^{n_{min} \times 1}$.

Theorem 3: [21] For $\mathbf{P}$ such that $[\mathbf{P}\Delta\mathbf{x}]_1 \neq 0$ for any non-zero value of $\Delta\mathbf{x} \in \{\mathbf{x}\text{-}\mathbf{x}'|\mathbf{x},\mathbf{x}' \in \mathcal{A}^{n_{min} \times 1}\}$, the diversity gain of the system is $n_t n_r$.

Proof: The instantaneous probability that a transmitted symbol vector $\mathbf{x}$ is falsely decoded to some other vector $\mathbf{x}'$ is given by

$$Pr\{\mathbf{x} \to \mathbf{x}'\} = Q\left(\sqrt{\frac{SNR}{2n_t E}}\|\mathbf{DP}(\mathbf{x}\text{-}\mathbf{x}')\|\right). \tag{5}$$

Let $\epsilon_{min} \triangleq \min_{\Delta\mathbf{x}}\{|[\mathbf{P}\Delta\mathbf{x}]_1|\}$, with $\Delta\mathbf{x} \neq \mathbf{O}_{n_{min} \times 1}$. So, the probability $P_e(\mathbf{x})$ that a transmitted vector $\mathbf{x}$ is falsely decoded is upper bounded as

$$P_e(\mathbf{x}) \leq (|\mathcal{A}|^{n_{min}} - 1) Q\left(\sqrt{\frac{SNR}{2n_t E}}\sigma_1 \epsilon_{min}\right), \tag{6}$$

where $\mathbf{D}(1,1) = \sigma_1$, the largest singular value of $\mathbf{H}$. Assuming that all the symbol vectors taking values from $\mathcal{A}^{n_{min} \times 1}$ are equally likely to be transmitted, the average instantaneous *word error probability* (WEP), dependent on $\mathbf{D}$ is given by

$$P_{e,\mathbf{D}} = \frac{1}{|\mathcal{A}|^{n_{min}}} \sum_{\mathbf{x} \in \mathcal{A}^{n_{min} \times 1}} P_e(\mathbf{x}). \tag{7}$$

Using (6) in (7),

$$P_{e,\mathbf{D}} \leq (|\mathcal{A}|^{n_{min}} - 1) Q\left(\sqrt{\frac{SNR}{2n_t E}}\sigma_1 \epsilon_{min}\right) = (|\mathcal{A}|^{n_{min}} - 1) Q\left(\sqrt{\left(\frac{\epsilon_{min}^2}{2n_t E}\right)\lambda_1 SNR}\right),$$

where $\lambda_1 = \sigma_1^2$. So, from Theorem 1 and Theorem 2, the average WEP P_e as $SNR \to \infty$ is given by

$$P_e \leq C.SNR^{-n_t n_r} + o\left(SNR^{-n_t n_r}\right), \tag{8}$$

where

$$C = (|\mathcal{A}|^{n_{min}} - 1)\frac{a_1(2n_t n_r - 1)(2n_t n_r - 3)\cdots 1}{2n_t n_r}\left(\frac{\epsilon_{min}^2}{2n_t E}\right)^{-n_t n_r},$$

with a_1 being a positive constant such that $f_{\lambda_1}(\lambda_1) = a_1\lambda_1^{n_t n_r - 1} + o\left(\lambda_1^{n_t n_r - 1}\right)$ as $\lambda_1 \to 0^+$. Note that in obtaining C, we have used the fact that $\Gamma(t+1) = t\Gamma(t)$ and $\Gamma(1/2) = \sqrt{\pi}$. Since $\epsilon_{min} > 0$, $C < \infty$ and from (8), the diversity gain achieved by the system is $n_t n_r$. ∎

An alternative proof of Theorem 3 has been presented in [21]. Since the steps of our proof are used in Section VI of this paper, and also for the sake of completeness, we have provided our version of the proof.

Note: The condition that $[\mathbf{P}\Delta\mathbf{x}]_1 \neq 0$ for any non-zero value of $\Delta\mathbf{x} \in \{\mathbf{x}\text{-}\mathbf{x}'|\mathbf{x},\mathbf{x}' \in \mathcal{A}^{n_{min}\times 1}\}$ is only *sufficient* to guarantee full-diversity. There might be several precoders which do not satisfy this condition but still give full-diversity. This will be elaborated in Section VI. Also note that in Theorem 3, the constraint is only on the first entry of $\mathbf{P}\Delta\mathbf{x}$. The other entries are allowed to be zeros.

Obtaining $\mathbf{P}$ such that $\epsilon_{min} \neq 0$ is not difficult. Choosing $\mathbf{P}$ to be $[\mathbf{G}\ \mathbf{O}_{n_r\times(n_t-n_r)}]^T$ (for $n_t > n_r$) or $\mathbf{G}$ (for $n_t \leq n_r$) for QAM constellations, where $\mathbf{G} \in \mathbb{R}^{n_{min}\times n_{min}}$ is the rotated $\mathbb{Z}^{n_{min}}$ lattice generator matrix with a non-zero product distance, as presented in [22], ensures that the diversity gain is $n_t n_r$. If $\mathcal{A}$ is a square QAM constellation of size M, the ML-decoding complexity is $\mathcal{O}\left(M^{\frac{n_{min}}{2}}\right)$, since all the n_{min} independent symbols are entangled in the decoding metric, but the real part of the symbol vector can be independently decoded from the imaginary part. This is possible because $\mathbf{G}$ is real-valued. In [21], complex-valued precoders are used to achieve full-diversity and they offer an ML-decoding complexity of $\mathcal{O}\left(M^{n_{min}}\right)$.

III. REVIEW OF LOW ML-DECODING COMPLEXITY PRECODERS

This section gives a brief overview of existing low-complexity precoders. The first precoder is called the E-d_{min} precoder [14], which is an extension of the MIMO precoder for $n_t = 2$ [15], developed for 4-QAM.

A. E-d_{min} precoder

The precoder $\mathbf{P}$ of size $n_{min} \times n_{min}$ (for $n_t > n_r$, the remaining $n_t - n_r$ rows of $\mathbf{P}$ are zeros) has the following structure

$$
\mathbf{P} = \begin{bmatrix}
\mathbf{M}_1(1,1) & & & & & & & \mathbf{M}_1(1,2) \\
& \mathbf{M}_2(1,1) & & & & & \mathbf{M}_2(1,2) & \\
& & \ddots & & & \iddots & & \\
& & & \mathbf{M}_{\frac{n_{min}}{2}}(1,1) & \mathbf{M}_{\frac{n_{min}}{2}}(1,2) & & & \\
& & & \mathbf{M}_{\frac{n_{min}}{2}}(2,1) & \mathbf{M}_{\frac{n_{min}}{2}}(2,2) & & & \\
& & \iddots & & & \ddots & & \\
& \mathbf{M}_2(2,1) & & & & & \mathbf{M}_2(2,2) & \\
\mathbf{M}_1(2,1) & & & & & & & \mathbf{M}_1(2,2)
\end{bmatrix}, \tag{9}
$$

where, if $\gamma_i \triangleq \tan^{-1}\left(\frac{\sigma_{n_{min}-i+1}}{\sigma_i}\right)$ is such that $0 < \gamma_i < \gamma_o$, then,

$$
\mathbf{M}_i = \sqrt{\frac{2n_t\tau_i^2}{n_{min}}} \begin{bmatrix} \sqrt{\frac{3+\sqrt{3}}{6}} & \sqrt{\frac{3-\sqrt{3}}{6}}e^{j\pi/12} \\ 0 & 0 \end{bmatrix} \tag{10}
$$

and if $\gamma_o \leq \gamma_i \leq \pi/4$,

$$
\mathbf{M}_i = \sqrt{\frac{n_t\tau_i^2}{n_{min}}} \begin{bmatrix} \cos\psi_i & 0 \\ 0 & \sin\psi_i \end{bmatrix} \begin{bmatrix} 1 & e^{j\pi/4} \\ -1 & e^{j\pi/4} \end{bmatrix},
$$

where,

$$
\psi_i = \tan^{-1}\left(\frac{\sqrt{2}-1}{\cos\gamma_i}\right), \quad \gamma_0 = \tan^{-1}\left(\sqrt{\frac{3\sqrt{3}-2\sqrt{6}+2\sqrt{2}-3}{3\sqrt{3}-2\sqrt{6}+1}}\right) \approx 0.3016
$$

and $\tau_i = \sqrt{\frac{n_{min}}{2}\left(\rho_i^2\delta(\gamma_i)\sum_{j=1}^{n_{min}}\frac{1}{\rho_j^2\delta(\gamma_j)}\right)^{-1}}$, with $\rho_i = \sqrt{\sigma_i^2 + \sigma_{n_{min}-i+1}^2}$ and

$$
\delta(\gamma_j) = \begin{cases} (1-\frac{1}{\sqrt{3}})\cos^2\gamma_j, & \text{if } 0 < \gamma_j < \gamma_o \\ \frac{(4-2\sqrt{2})\cos^2\gamma_j\sin^2\gamma_j}{1+(2-2\sqrt{2})\cos^2\gamma_j}, & \text{otherwise.} \end{cases}
$$

The precoder essentially entangles the virtual subchannels with index i and $n_{min} - i + 1$, $i = 1, 2,$ $\cdots, n_{min}/2$[3]. Such a scheme will have an ML-decoding complexity of $\mathcal{O}\left(M\sqrt{M}\right)$. It has been shown that the scheme guarantees a diversity gain equal to $(n_t - \frac{n_{min}}{2} + 1)(n_r - \frac{n_{min}}{2} + 1)$. Also, the precoder is optimal among precoders based on the SVD of the channel for $n_{min} = 2$ and 4-QAM [15].

---

[3] for odd valued n_{min}, $\frac{n_{min}}{2}$ is replaced by $\lfloor\frac{n_{min}}{2}\rfloor$ and the $\left(\lfloor\frac{n_{min}}{2}\rfloor + 1\right)^{th}$ subchannel is left unpaired.

B. X-precoder

The X-precoder has the same structure as in (9), with the matrices $\mathbf{M}_i$ given as

$$\mathbf{M}_i = \sqrt{\frac{n_t}{n_{min}}} \begin{bmatrix} \cos\theta_i & -\sin\theta_i \\ \sin\theta_i & \cos\theta_i \end{bmatrix},$$

where, for 4-QAM,

$$\theta_i = \begin{cases} \pi/4, & \text{if } \gamma_i \geq \pi/3 \\ \tan^{-1}\left(\frac{1-\tan^2\gamma_i - \sqrt{1+\tan^4\gamma_i - 3\tan^2\gamma_i}}{\tan^2\gamma_i}\right) & \text{otherwise.} \end{cases}$$

This scheme has also been shown to guarantee a diversity gain equal to $(n_t - \frac{n_{min}}{2} + 1)(n_r - \frac{n_{min}}{2} + 1)$, but has an ML-decoding complexity of $\mathcal{O}\left(\sqrt{M}\right)$ only (refer Subsection IV-D for details). However, it is expected to lose out in performance for 4-QAM when compared with the E-d_{min} precoder, since it is not optimal. Also, an explicit expression for the precoder when $M > 4$ does not exist.

C. Y-precoder

The Y-precoder [16] has the Y-structure but it uses a displacement vector and its precoded symbol vector $\mathbf{s}$ can be written as

$$\mathbf{s} = \mathbf{V}(\mathbf{P}\mathbf{x} + \mathbf{u}), \tag{11}$$

where, $\mathbf{u}$ is the displacement vector. The precoded vector can also be expressed as

$$\mathbf{s} = \mathbf{V}\mathbf{P}_{eff}\mathbf{x}_{eff},$$

where, $\mathbf{P}\mathbf{x} + \mathbf{u} = \mathbf{P}_{eff}\mathbf{x}_{eff}$, with $\mathbf{P}_{eff}$ and $\mathbf{x}_{eff}$ being the effective precoder and the effective symbol vector, respectively. These are defined as

$$\mathbf{P}_{eff} = \text{diag}\left(a_1, a_2, \cdots, a_{\frac{n_{min}}{2}}, b_{\frac{n_{min}}{2}}, \cdots, b_2, b_1\right)$$

where,

$$(a_i, b_i) = \begin{cases} \left(\sqrt{\frac{3n_t}{n_r(M^2-1)}}, 0\right), & \text{if } \beta_i^2 \geq \frac{M^2-1}{3} \\ \left(\sqrt{\frac{n_t}{3n_r(\beta_i^2+M')}}, \beta_i\sqrt{\frac{n_t}{n_r(\beta_i^2+M')}}\right) & \text{otherwise,} \end{cases}$$

and $M' = \frac{M^2-1}{9}$ and $\beta_i = \frac{\sigma_i}{\sigma_{n_{min}-i+1}}$. The constellation $\mathcal{A} \in \mathbb{Z}^{2\times 1}$ of size M is two-dimensional with the signal vectors (not to be confused with the symbol vector $\mathbf{x}_{eff}$) $\mathbf{z}_l$, $l = 1, 2, \cdots, M$ defined as

$$\mathbf{z}_l = \begin{bmatrix} 2l - M - 1 \\ (-1)^l \end{bmatrix}$$

and the symbol vector that is associated with the $(i, n_{min} - i + 1)$ subchannel pairing is $\mathbf{s}_i \triangleq \mathbf{v}_i + j\mathbf{v}_{n_{min}-i+1}$, with $\mathbf{v}_i, \mathbf{v}_{n_{min}-i+1} \in \mathcal{A}$, $i = 1, 2, \cdots, n_{min}/2$. Hence,

$$\mathbf{x}_{eff} = \left[[\mathbf{s}_1]_1, [\mathbf{s}_2]_1, \cdots, [\mathbf{s}_{\frac{n_{min}}{2}}]_1, [\mathbf{s}_{\frac{n_{min}}{2}}]_2, \cdots, [\mathbf{s}_2]_2, [\mathbf{s}_1]_2 \right]^T.$$

So, the effective precoder of the Y-precoder is a diagonal matrix, while $\mathbf{P}$, as given in (11), has the 'Y' structure. The Y-precoder has been shown to have better error performance than the X-precoder for "ill-conditioned" channels, i.e., for low values of $\frac{\sigma_{n_{min}-i+1}}{\sigma_i}$, $i = 1, 2, \cdots, n_{min}/2$, while for well-conditioned channels, the X-precoder has better error performance. However, the Y-precoder has lower ML-decoding complexity, which is $\mathcal{O}(1)$. Hence, among all existing precoders, the Y-precoder has the least ML-decoding complexity while the E-d_{min} precoder has the best performance for 4-QAM.

IV. SVD-BASED, APPROXIMATELY OPTIMAL, REAL-VALUED PRECODER FOR $n_t = 2$

In this section, we propose a real-valued precoder for 2 transmit antennas and QAM constellations. The precoder is approximately optimal among the SVD based real-valued precoders for QAM constellations. The primary advantage of this precoder over the complex-valued optimal precoder [15] is that it is much easier to find the entries of the precoder for larger constellations, since it has only 2 parameters that need to be searched for, while the complex-valued precoder has 3 parameters. Without loss of generality, we consider 2 receive antennas and 2 transmit antennas, for which $\mathbf{D}$ in (3) can be expressed as

$$\mathbf{D} = \rho \begin{bmatrix} \cos\gamma & 0 \\ 0 & \sin\gamma \end{bmatrix},$$

where $\rho = \sqrt{\sigma_1^2 + \sigma_2^2}$ and $\gamma = \tan^{-1}(\frac{\sigma_2}{\sigma_1})$. Clearly, $0 < \gamma \leq \pi/4$. Let

$$E_{min}(\mathbf{P}) \triangleq \min_{\Delta\mathbf{x} \neq \mathbf{O}_{2\times 1}} \left\{ \|\mathbf{D}\mathbf{P}\Delta\mathbf{x}\|^2, \quad \Delta\mathbf{x} \in \{\mathbf{x} - \mathbf{x}' \mid \mathbf{x}, \mathbf{x}' \in \mathcal{A}^{2\times 1}\} \right\}. \tag{12}$$

From (5), the optimal precoder is given by $\mathbf{P}^{opt} = \underset{\mathbf{P}}{\arg\max}\{E_{min}(\mathbf{P})\}$, which may or may not be unique. In [15], $\mathbf{P}^{opt} \in \mathbb{C}^{2\times 2}$ was obtained for 4-QAM as follows. Using SVD, $\mathbf{P} \in \mathbb{C}^{2\times 2}$ can be written as

$\mathbf{P} = \mathbf{A}\mathbf{\Sigma}\mathbf{B^H}$, where $\mathbf{A}$ is a unitary matrix of size 2×2 and

$$\mathbf{\Sigma} = \sqrt{2} \begin{bmatrix} \cos\psi & 0 \\ 0 & \sin\psi \end{bmatrix}, \quad \mathbf{B}^H = \begin{bmatrix} \cos\theta & -\sin\theta \\ \sin\theta & \cos\theta \end{bmatrix} \begin{bmatrix} 1 & 0 \\ 0 & e^{j\phi} \end{bmatrix}. \tag{13}$$

For QAM constellations, because of the symmetry associated with the constellation, $0 \leq \theta \leq \pi/4$, $0 \leq \psi \leq \pi/2$ and $0 \leq \phi \leq \pi/2$. It was shown in [15] that $\mathbf{A}$ can be taken to be identity without affecting the optimality. Using numerical search, the optimal values for θ, ψ and ϕ were found out for 4-QAM. However, there are two major obstacles when this method is used for larger QAM constellations. Firstly, numerical search becomes practically hard for larger constellations due to the fact that there are three parameters to be searched for. Secondly, numerical searches do not give a closed form expression for the optimal angles and the method employed in [15] to obtain closed form expressions for the optimal angles for 4-QAM is not amenable for application to larger QAM constellations. Due to these limitations, we look for a real-valued optimal precoder which also naturally offers lower ML-decoding complexity (this is elaborated in Subsection IV-D). A real-valued precoder can be expressed as $\mathbf{P}(\psi, \theta) = \mathbf{A}\mathbf{\Sigma}\mathbf{B}^T$ where $\mathbf{A}$ can be taken to be identity without affecting optimality and

$$\mathbf{\Sigma} = \sqrt{2} \begin{bmatrix} \cos\psi & 0 \\ 0 & \sin\psi \end{bmatrix}, \quad \mathbf{B} = \begin{bmatrix} \cos\theta & \sin\theta \\ -\sin\theta & \cos\theta \end{bmatrix}.$$

Note that there are only two parameters to be searched for. Our approach towards finding the optimal precoders is also based on numerical search, but the method to obtain closed form expressions for the optimal angles is novel and easily applicable for any M-QAM. However, since this method is based on numerical search, it is not known if the angles are exactly optimal. Finding the exactly optimal values of θ and ψ as a function of γ involves an *exhaustive* search over the range of θ and ψ, which is practically impossible. However, a numerical search, with θ and ψ varying in very small increments, gives the values of θ and ψ, which we denote by θ^* and ψ^*, respectively, such that $E_{min}(\mathbf{P}(\psi^*, \theta^*))$ is nearly equal to $E_{min}(\mathbf{P}^{opt})$, with $\mathbf{P}^{opt}$ being the optimal real-valued precoder. For this reason, we call our precoder approximately optimal.

A square QAM signal set (not necessarily Gray coded) of size M is given by

$$\mathcal{A}_{M-QAM} = \{a + jb \mid a, b \in \mathcal{A}_{\sqrt{M}-PAM}\}, \tag{14}$$

where $\mathcal{A}_{\sqrt{M}-PAM} = \{2i - \sqrt{M} - 1, i = 1, 2, \cdots, \sqrt{M}\}$ is a PAM constellation of size $\sqrt{M}$. Let

$$\mathbf{F}(\gamma, \psi, \theta) \triangleq \begin{bmatrix} \cos\gamma & 0 \\ 0 & \sin\gamma \end{bmatrix} \begin{bmatrix} \cos\psi & 0 \\ 0 & \sin\psi \end{bmatrix} \begin{bmatrix} \cos\theta & -\sin\theta \\ \sin\theta & \cos\theta \end{bmatrix},$$

and

$$\delta(\gamma, \mathcal{A}) = \max_{(\psi, \theta)} \left\{ \min_{\Delta\mathbf{x} | \Delta\mathbf{x} \neq \mathbf{O}_{2\times 1}} \left\{ \|\mathbf{F}(\gamma, \psi, \theta)\Delta\mathbf{x}\|^2, \quad \Delta\mathbf{x} \in \{\mathbf{x}, \mathbf{x}' \mid \mathbf{x}, \mathbf{x}' \in \mathcal{A}^{2\times 1}\} \right\} \right\}, \tag{15}$$

where, for our numerical search, we take $\psi = \Delta.k, \; k = 1, 2, \cdots, \lfloor \frac{\pi}{2\Delta} \rfloor, \; \theta = \Delta.k, \; k = 1, 2, \cdots, \lfloor \frac{\pi}{4\Delta} \rfloor$, with Δ being the increment size, taken to be 0.001 radians for our searches. Let

$$(\psi^*, \theta^*) = \underset{(\psi, \theta)}{\operatorname{argmax}} \left\{ \min_{\Delta\mathbf{x}, \Delta\mathbf{x} \neq \mathbf{O}_{2\times 1}} \left\{ \|\mathbf{F}(\gamma, \psi, \theta)\Delta\mathbf{x}\|^2 \right\} \right\}. \tag{16}$$

We note that for M-QAM, $E_{min}(\mathbf{P}(\psi^*, \theta^*)) = 2\rho^2\delta\left(\gamma, \mathcal{A}_{M-QAM}\right) = 2\rho^2\delta\left(\gamma, \mathcal{A}_{\sqrt{M}-PAM}\right)$. Hence, we only need to search for θ^* and ψ^* for which $\delta(\gamma, \mathcal{A}_{\sqrt{M}-PAM})$ is obtained. Note that this simplification of the search to only a $\sqrt{M}$-PAM is possible since $\mathbf{F}(\gamma, \psi, \theta)$ is real-valued. This is another huge advantage over the complex-valued precoder, which does not enjoy this benefit. Henceforth, θ^* and ψ^* are used to denote the approximately optimal angles of θ and ψ. Due to our choice of the increment size, one can safely say that $\left(E_{min}(\mathbf{P}^{opt}) - E_{min}(\mathbf{P}(\theta^*, \psi^*))\right) < \kappa.E_{min}(\mathbf{P}^{opt})$, where κ is a very small fraction of the order of 10^{-3}.

The search results reveal that θ^* as a function of γ can be written as

$$\theta^* = \sum_{k=1}^{n} \theta_k^* \left(u(\gamma - \gamma_k') - u(\gamma - \gamma_k' - w_k) \right), \tag{17}$$

where $\theta_k^*, k = 1, \cdots, n$, are constants, n is the finite number of different values θ^* takes, γ_k' is the value of γ at which θ^* changes from θ_{k-1}^* to θ_k^*, with $\gamma_1' = 0$, $\theta_0^* = 0$, $w_k = \gamma_{k+1}' - \gamma_k'$ and $\gamma_{n+1}' = \pi/4$. The search results also reveal that ψ^* cannot be expressed as a weighted sum of shifted step functions and hence a closed form expression needs to be obtained analytically. To obtain this, we first obtain θ^* as follows.

A. Calculating θ^*

For M-QAM, in order to obtain θ^* and ψ^*, as given by (16), the entries of $\Delta\mathbf{x}$ take values from $\left\{ 2\left(-\sqrt{M} + i\right), i = 1, 2, \cdots, 2\sqrt{M} - 1 \right\}$. Let $p, q \in \{-\sqrt{M} + i, i = 1, 2, \cdots, 2\sqrt{M} - 1\}$ be such that

$$4\|\mathbf{F}\left(\gamma, \psi^*, \theta^*\right)[p \; q]^T\|^2 = \delta(\gamma, \mathcal{A}_{M-QAM}) = \delta(\gamma, \mathcal{A}_{\sqrt{M}-PAM}). \tag{18}$$

The numerical searches done for 5 QAM constellations - 4-/16-/64-/256-/1024-QAM reveal that

1) there are two distinct (p,q) pairs for which (18) is satisfied when $0 < \gamma \le \gamma_2'$, where γ_2' is as defined in (17). These are $(0,1)$ and $(1, \sqrt{M} - 1)$. Also $\psi^* = 0$ in this range of γ.

2) There are three distinct (p,q) pairs for which (18) is satisfied when $\gamma_k' \le \gamma \le \gamma_{k+1}'$, $k = 2, \cdots, n$.

Let

$$\varepsilon(p, q, \theta^*, \psi^*) \triangleq \cos^2 \gamma \cos^2(\psi^*) (p \cos(\theta^*) - q \sin(\theta^*))^2 + \sin^2 \gamma \sin^2(\psi^*) (q \cos(\theta^*) + p \sin(\theta^*))^2.$$

So, for $0 < \gamma \le \gamma_2'$, we have

$$\varepsilon(0, 1, \theta_1^*, 0) = \varepsilon(1, \sqrt{M} - 1, \theta_1^*, 0),$$

solving which we obtain $\theta_1^* = \tan^{-1} \frac{1}{\sqrt{M}}$. The other solution, which is $\theta_1^* = \tan^{-1}\left(\frac{1}{\sqrt{M}-2}\right)$, is ruled out since it has been observed that $E_{min}\left(\mathbf{P}\left(0, \tan^{-1}\left(1/\sqrt{M}\right)\right)\right) > E_{min}\left(\mathbf{P}\left(0, \tan^{-1}\left(1/(\sqrt{M} - 2)\right)\right)\right)$ for $0 < \gamma \le \gamma_2'$. For $\gamma_k' \le \gamma \le \gamma_{k+1}'$, $k = 2, \cdots, n$, we have

$$\varepsilon(p_1, q_1, \theta_k^*, \psi^*) = \varepsilon(p_2, q_2, \theta_k^*, \psi^*) = \varepsilon(p_3, q_3, \theta_k^*, \psi^*),$$

where (p_1, q_1), (p_2, q_2) and (p_3, q_3) are the three pairs for which (18) is satisfied. Solving them, we arrive at

$$\tan^2 \gamma \tan^2(\psi^*) = 1 + \frac{p_1^2 + q_1^2 - p_2^2 - q_2^2}{(p_2 q_2 - p_1 q_1) \sin(2\theta_k^*) + (q_2^2 - q_1^2) \cos^2(\theta_k^*) + (p_2^2 - p_1^2) \sin^2(\theta_k^*)}, \quad (19)$$

$$\tan^2 \gamma \tan^2(\psi^*) = 1 + \frac{p_1^2 + q_1^2 - p_3^2 - q_3^2}{(p_3 q_3 - p_1 q_1) \sin(2\theta_k^*) + (q_3^2 - q_1^2) \cos^2(\theta_k^*) + (p_3^2 - p_1^2) \sin^2(\theta_k^*)}. \quad (20)$$

Equating (19) and (20), we obtain

$$(a_1 d_2 - a_2 d_1) \tan^2(\theta_k^*) + 2(a_1 b_2 - a_2 b_1) \tan(\theta_k^*) + a_1 c_2 - a_2 c_1 = 0, \quad (21)$$

where $a_1 = p_1^2 + q_1^2 - p_2^2 - q_2^2$, $b_1 = p_2 q_2 - p_1 q_1$, $c_1 = q_2^2 - q_1^2$, $d_1 = p_2^2 - p_1^2$, $a_2 = p_1^2 + q_1^2 - p_3^2 - q_3^2$, $b_2 = p_3 q_3 - p_1 q_1$, $c_2 = q_3^2 - q_1^2$ and $d_2 = p_3^2 - p_1^2$. Equation (21) has been observed to have only one solution in the range $(0, \pi/4)$. This solution gives θ_k^*.

B. Calculating ψ^*

As mentioned before, $\psi^* = 0$ for $0 < \gamma \le \gamma_2'$. In order to obtain ψ^* for $\gamma_k' \le \gamma \le \gamma_{k+1}'$, $k = 2, \cdots, n$, we note from (19) and (20) that $\tan^2 \gamma \tan^2(\psi^*)$ is constant in that range of γ and hence,

$$\psi^* = \tan^{-1}\left(\frac{\sqrt{A_k}}{\tan\gamma}\right), \tag{22}$$

where A_k is given by the R.H.S of (19) (or (20)).

C. Calculating γ'_k

Having obtained θ^* and ψ^*, we proceed to find the exact values of γ'_k, $k = 2, \cdots, n$ as follows. For convenience, let $\psi^*(\theta^*_k, \gamma) \triangleq \psi^*$ (given by (22)) for $\gamma'_k \leq \gamma \leq \gamma'_{k+1}$, $k = 1, \cdots, n$. Since θ^* is discontinuous at γ'_k, where it makes a transition from θ^*_{k-1} to θ^*_k, $k \geq 2$, we have

$$\varepsilon\left(p_{k-1}, q_{k-1}, \theta^*_{k-1}, \psi^*(\theta^*_{k-1}, \gamma'_k)\right) = \varepsilon\left(p_k, q_k, \theta^*_k, \psi^*(\theta^*_k, \gamma'_k)\right),$$

where the pairs (p_{k-1}, q_{k-1}) and (p_k, q_k) satisfy (18) for $\gamma'_{k-1} \leq \gamma \leq \gamma'_k$ and $\gamma'_k \leq \gamma \leq \gamma'_{k+1}$, respectively. So, we have

$$\cos^2\left(\psi^*(\theta^*_{k-1}, \gamma'_k)\right) = \cos^2\left(\psi^*(\theta^*_k, \gamma'_k)\right)\left(\frac{c + A_k d}{a + A_{k-1} b}\right), \tag{23}$$

$$\sin^2\left(\psi^*(\theta^*_{k-1}, \gamma'_k)\right) = \sin^2\left(\psi^*(\theta^*_k, \gamma'_k)\right)\left(\frac{A_{k-1}}{A_k}\right)\left(\frac{c + A_k d}{a + A_{k-1} b}\right), \tag{24}$$

where $a = \left(p_{k-1}\cos\left(\theta^*_{k-1}\right) - q_{k-1}\sin\left(\theta^*_{k-1}\right)\right)^2$, $b = \left(q_{k-1}\cos\left(\theta^*_{k-1}\right) + p_{k-1}\sin\left(\theta^*_{k-1}\right)\right)^2$, $c = \left(p_k\cos\left(\theta^*_k\right) - q_k\sin\left(\theta^*_k\right)\right)^2$, $d = \left(q_k\cos\left(\theta^*_k\right) + p_k\sin\left(\theta^*_k\right)\right)^2$, and as explained in Subsection IV-B, A_{k-1} and A_k are constants given by $A_{k-1} = \tan^2\gamma\tan^2\left(\psi^*(\theta^*_{k-1}, \gamma)\right)$ for $\gamma'_{k-1} \leq \gamma \leq \gamma'_k$, $A_k = \tan^2\gamma\tan^2\left(\psi^*(\theta^*_k, \gamma)\right)$ for $\gamma'_k \leq \gamma \leq \gamma'_{k+1}$. Solving (23) and (24), we obtain,

$$\psi^*(\theta^*_k, \gamma'_k) = \sin^{-1}\sqrt{\left(\frac{A_{k-1}}{A_k} - 1\right)^{-1}\left(\frac{a + A_{k-1}b}{c + A_k d} - 1\right)}. \tag{25}$$

Using (22) and (25),

$$\gamma'_k = \tan^{-1}\left(\frac{\sqrt{A_k}}{\tan\left(\psi^*\left(\theta^*_k, \gamma'_k\right)\right)}\right).$$

The value of $\delta(\gamma, \mathcal{A}_{M-QAM})$ as defined in (15) for $\gamma'_k \leq \gamma \leq \gamma'_{k+1}$ is given by

$$\delta(\gamma, \mathcal{A}_{M-QAM}) = \sin^2\gamma\left(\frac{c + A_k d}{A_k + \tan^2\gamma}\right), \tag{26}$$

where $c = \left(p_k\cos\left(\theta^*_k\right) - q_k\sin\left(\theta^*_k\right)\right)^2$, $d = \left(q_k\cos\left(\theta^*_k\right) + p_k\sin\left(\theta^*_k\right)\right)^2$, with (p_k, q_k) any of the (p, q) pairs satisfying (18).

Table I presents the values of θ^* for different values of γ for 4-QAM, 16-QAM, 64-QAM, 256-QAM

and 1024-QAM. The value of the constants $\tan\gamma\tan(\psi^*)$ and the corresponding pairs (p,q) for which (18) is satisfied are also tabulated. Except for the case of 4-QAM, the values presented in Table I are the approximately optimal values rounded off to the fourth decimal. This has been done since it is very cumbersome to express them in the exact form. All angles are expressed in radians. Noting the values of θ^* for 4-QAM, it is natural to believe that the angles tabulated are optimal for 4-QAM. Also, it can be noted that for every subsequent larger constellation, θ^* differs from its corresponding values for the lower-sized constellation only at low values of γ, meaning which the numerical search need not be done over the entire range of γ as the size of the constellation increases. The plots of $\delta(\gamma, \mathcal{A}_{M-QAM})$ as a function of γ for the different unnormalized QAM constellations are given in Fig. 1. The curves for 256- and 1024-QAM appear to coincide, since they differ only at extremely low values of γ. In Fig. 2, the plots[4] of $\delta(\gamma, \mathcal{A})$ for the E-d_{min} precoder, the proposed precoder, the X-precoder and the Y-precoder are given for $M = 4$ with the same power constraint for all the precoders as for our precoder. As was expected, the E-d_{min} precoder has the best values of $\delta(\gamma, \mathcal{A})$ over the entire range of γ while our precoder has better values of $\delta(\gamma, \mathcal{A})$ than the X- and Y-precoders. Fig. 3 and Fig. 4 show the plots of $\delta(\gamma, \mathcal{A})$ for our precoder, the X-precoder and the Y-precoder for $M = 16$ and $M = 64$, respectively. For the X-precoder, the plots were obtained using numerical searches to obtain the approximately optimal angle for each value of γ in the range $(0, \pi/4)$, with γ increasing in step sizes of 0.001. Note that for low values of γ, our precoder and the Y-precoder have identical $\delta(\gamma, \mathcal{A})$, which is because both transmission schemes are effectively the same in this range of γ. With an increase in the constellation size, the Y-precoder has increasingly lower values of $\delta(\gamma, \mathcal{A})$ than that of our precoder and the X-precoder at higher values of γ. It is also clear from the plots that the Y-precoder is expected to have better error performance than the X-precoder only for ill-conditioned channels, i.e., for low values of γ.

D. ML-decoding complexity

We make use of the following lemma to analyze the ML-decoding complexity of our precoder.

Lemma 1: For symbols x_1 and x_2 taking values from $\mathcal{A}_{M-QAM}$, the symbol $ax_1 + bx_2$ takes values from $\mathcal{A}_{M^2-QAM}$ if $a = \sqrt{M}$, $b = 1$ or $b = \sqrt{M}$, $a = 1$.

Proof: Firstly, $\mathcal{A}_{M-QAM}$ represents the standard, unnormalized M-QAM constellation, as given in (14). Let $\sqrt{M}\mathcal{A}_{M-QAM}$ denote the M-QAM constellation scaled by $\sqrt{M}$. So, the distance between any

---

[4]In all the plots, the E-d_{min} precoder, our precoder and the X-precoder use M-QAM, while the Y-precoder uses a two-dimensional codebook of size M, as defined in [16].

two adjacent signal points on the same vertical or horizontal line of $\sqrt{M}\mathcal{A}_{M-QAM}$ is $2\sqrt{M}$. Now, the constellation given by

$$\mathcal{A} = \left\{ \sqrt{M}x_1 + x_2 \mid x_1, x_2 \in \mathcal{A}_{M-QAM} \right\} \tag{27}$$

can be viewed to be obtained by replacing every element of $\sqrt{M}\mathcal{A}_{M-QAM}$ by the entire constellation $\mathcal{A}_{M-QAM}$ such that the origin of $\mathcal{A}_{M-QAM}$ is the signal point being replaced. Hence, $\mathcal{A}$ has M^2 signal points and a QAM structure, and the distance between adjacent points on the same vertical or horizontal line is 2. Therefore, $\mathcal{A}$ is an M^2-QAM. ∎

The following theorem gives the ML-decoding complexity of the precoder.

Theorem 4: For the proposed precoder, the following claims hold.

1) The ML-decoding complexity is $\mathcal{O}(\sqrt{M})$, when $\gamma'_k \le \gamma \le \gamma'_{k+1}$, $k = 2, 3, \cdots, n$.

2) The ML-decoding complexity is the same as that of a real scalar channel when $0 < \gamma \le \gamma'_2$, with no exhaustive search over all the signal points required.

Proof: These claims are proved below.

Case 1 : $\gamma'_k \le \gamma \le \gamma'_{k+1}, \quad k = 2, 3, \cdots, n.$

In this case, the decoded signal vector $\check{\mathbf{x}}$ is

$$\check{\mathbf{x}} = \underset{\mathbf{x} \in \mathcal{A}^{2 \times 1}_{M-QAM}}{\operatorname{argmin}} \left\{ \left\| \mathbf{y}' - \sqrt{\frac{SNR}{2E_M}} \mathbf{DPx} \right\|^2 \right\} = \underset{\mathbf{x} \in \mathcal{A}^{2 \times 1}_{M-QAM}}{\operatorname{argmin}} \left\{ \left\| \mathbf{y}'' - \sqrt{\frac{SNR}{2E_M}} \mathbf{Rx} \right\|^2 \right\}, \tag{28}$$

where $\mathbf{y}'$, $\mathbf{D}$ and $\mathbf{P}$ are as defined in (3), $E_M = 2(M-1)/3$ is the average energy of an M-QAM and $\mathbf{y}'' = \mathbf{Q}^T\mathbf{y}'$, with $\mathbf{Q}$ and $\mathbf{R}$ obtained on the QR-decomposition of $\mathbf{DP}$. Since $\mathbf{D}$ and $\mathbf{P}$ are real-valued, (28) can be written as $\check{\mathbf{x}} = \check{\mathbf{x}}_I + j\check{\mathbf{x}}_Q$, where

$$\check{\mathbf{x}}_I = \underset{\mathbf{x}_I \in \mathcal{A}^{2 \times 1}_{\sqrt{M}-PAM}}{\operatorname{argmin}} \left\{ \left\| \mathbf{y}''_I - \sqrt{\frac{SNR}{2E_M}} \mathbf{Rx}_I \right\|^2 \right\}, \quad \check{\mathbf{x}}_Q = \underset{\mathbf{x}_Q \in \mathcal{A}^{2 \times 1}_{\sqrt{M}-PAM}}{\operatorname{argmin}} \left\{ \left\| \mathbf{y}''_Q - \sqrt{\frac{SNR}{2E_M}} \mathbf{Rx}_Q \right\|^2 \right\},$$

with

$$\mathbf{y}'' = \mathbf{y}''_I + j\mathbf{y}''_Q = \left[y''_{1I} + jy''_{1Q}, \ y''_{2I} + jy''_{2Q} \right]^T, \quad \check{\mathbf{x}} \triangleq \check{\mathbf{x}}_I + j\check{\mathbf{x}}_Q = \left[\check{x}_{1I} + j\check{x}_{1Q}, \ \check{x}_{2I} + j\check{x}_{2Q} \right]^T.$$

To obtain $\check{\mathbf{x}}_I$, instead of using a 2-dimensional real sphere decoder, we do the following. For each possible value of $x_{2I} \in \mathcal{A}_{\sqrt{M}-PAM}$, the corresponding value of x_{1I} is evaluated as

$$x_{1I} = \min \left(\max \left(2 . \operatorname{rnd} \left[\frac{u+1}{2} \right] - 1, -\sqrt{M} + 1 \right), \sqrt{M} - 1 \right), \tag{29}$$

where

$$u = \frac{\sqrt{\frac{2E_M}{SNR}} y''_{1I} - \mathbf{R}(1,2) x_{2I}}{\mathbf{R}(1,1)}$$

and $\check{\mathbf{x}}_I$ is given by that (x_{1I}, x_{2I}) pair that minimizes

$$f(\mathbf{x}_I) = \left\| \mathbf{y}''_I - \sqrt{\frac{SNR}{2E_M}} \mathbf{R} \mathbf{x}_I \right\|^2 .$$

So, there are only $\sqrt{M}$ searches (for $\sqrt{M}$ possibilities for x_{2I}) involved in minimizing the ML-metric. The operation shown on the R.H.S of (29) quantizes x_{1I} to its nearest possible value for a fixed x_{2I}. This is made possible due to the structure of M-QAM which is a Cartesian product of two $\sqrt{M}$-PAM constellations. The same method can be applied to obtain $\check{\mathbf{x}}_Q$. So, the ML-decoding complexity is $\mathcal{O}(\sqrt{M})$.

Case 2: $0 < \gamma \le \gamma'_2$.

From Table I and also as was pointed out earlier, for $0 < \gamma \le \gamma'_2$, $\psi^* = 0$ and $\theta^* = \tan^{-1}\left(\frac{1}{\sqrt{M}}\right)$. This means that transmission is made only on the first virtual subchannel and the received signal of interest, with regard to (3), can be expressed as

$$y'_1 = ax' + n'_1,$$

where n'_1 is the first element of $\mathbf{n}'$, $a = \sqrt{\sigma_1^2 SNR/((M+1)E_M)}$ and $x' = \sqrt{M} x_1 + x_2$, where x_1 and x_2 take values from $\mathcal{A}_{M-QAM}$. From Lemma 1, x' takes values[5] from $\mathcal{A}_{M^2-QAM}$. So, in the first step, x' is decoded to obtain $\check{x}' = \check{x}'_I + j\check{x}'_Q$ by quantizing, where $\check{x}'_I$ and $\check{x}'_Q$ are given by

$$\check{x}'_I = \min\left(\max\left(2.\text{rnd}\left[\frac{\frac{y'_{1I}}{a}+1}{2}\right] - 1, -M+1\right), M-1\right),$$

$$\check{x}'_Q = \min\left(\max\left(2.\text{rnd}\left[\frac{\frac{y'_{1Q}}{a}+1}{2}\right] - 1, -M+1\right), M-1\right).$$

From $\check{x}'$, x_1 is decoded to obtain $\check{x}_1 = \check{x}_{1I} + j\check{x}_{1Q}$, with $\check{x}_{1I}$ and $\check{x}_{1Q}$ given by

$$\check{x}_{1I} = \text{sgn}(\check{x}'_I)\left(2\left\lceil\frac{|\check{x}'_I|}{2\sqrt{M}}\right\rceil - 1\right), \quad \check{x}_{1Q} = \text{sgn}(\check{x}'_Q)\left(2\left\lceil\frac{|\check{x}'_Q|}{2\sqrt{M}}\right\rceil - 1\right) \tag{30}$$

---

[5]From a bit error rate point of view, it is advisable to transmit a symbol x_1 alone on the first virtual subchannel, with x_1 taking values from a Gray coded M^2-QAM. This is because the constellation given by (27) will not be Gray coded. However, with a view of minimizing the word error rate, transmission of $x' = \sqrt{M} x_1 + x_2$, with x_1 and x_2 taking values from $M-$QAM, is as good a strategy as transmitting x_1 alone, with x_1 taking values from a Gray coded M^2-QAM.

and x_2 is decoded to obtain $\check{x}_2 = \check{x}_{2I} + j\check{x}_{2Q}$, with $\check{x}_{2I}$ and $\check{x}_{2Q}$ given by

$$\check{x}_{2I} = \check{x}'_I - \sqrt{M}\check{x}_{1I}, \quad \check{x}_{2Q} = \check{x}'_Q - \sqrt{M}\check{x}_{1Q}. \tag{31}$$

Note that the operations shown in (30) and (31) together perform the inverse of the function given by

$$f(\check{x}_{1I}, \check{x}_{1Q}, \check{x}_{2I}, \check{x}_{2Q}) = \sqrt{M}(\check{x}_{1I} + j\check{x}_{1Q}) + (\check{x}_{2I} + j\check{x}_{2Q})$$

for $\check{x}_{1I}, \check{x}_{1Q}, \check{x}_{2I}, \check{x}_{2Q} \in A_{\sqrt{M}-PAM}$. Therefore, decoding x_1 and x_2 requires no exhaustive search over the M signal points of the constellation. ∎

It has to be pointed out that the advantage of not having to search over any of the signal points when $0 < \gamma \le \gamma'_2$ is unique to the proposed real-valued precoder and not obtainable for the case of the complex-valued optimal precoder [15] for 4-QAM, for which the effective constellation when $0 < \gamma \le 0.3016$ appears like a $\pi/12$ rotated QAM constellation (it is not exactly a rotated QAM constellation, however. Hence, when, $0 < \gamma \le 0.3016$, even the sphere decoder cannot be used, since the effective constellation is not a lattice).

V. EXTENSION FOR $n_t > 2$

For the case of two transmit antennas, it is possible to obtain SVD-based, approximately optimal precoders (complex-valued precoder for 4-QAM, real-valued precoder for any M-QAM). Such precoders are defined by two or three parameters, depending on whether the precoder is real-valued or complex-valued, respectively. However, such an approach cannot be taken for the case of $n_t > 2$, since, even for $n_t = 3$, an optimal precoder would be defined by as many as 5 parameters, ruling out the possibility of a computer search even for 4-QAM. So, a more practical way of obtaining a precoder with a reasonable error performance is to pair the ith and the $(n_{min} - i + 1)^{th}$ subchannels along with the ith and the $(n_{min} - i + 1)^{th}$ symbols, $i = 1, 2 \cdots, n_{min}/2$ and use the precoding scheme for 2 transmit antennas for this pair. This method of pairing has been shown to be the best in [14] and has also been adopted in [16]. The precoder would then have an 'X' structure, as in (9). For the ith subchannel pairing, $\gamma_i \triangleq \tan^{-1}(\sigma_{n_{min}-i+1}/\sigma_i)$, $\rho_i = \sqrt{\sigma_i^2 + \sigma_{n_{min}-i+1}^2}$ and

$$\delta(\gamma_i, \mathcal{A}_{M-QAM}) = \sin^2 \gamma_i \left(\frac{c_i + A_{ki}d_i}{A_{ki} + \tan^2 \gamma_i} \right), \tag{32}$$

where c_i, b_i and A_{ki} are as defined in the previous section without the subscript i (refer to (26)) and depend on γ_i and M. Proceeding on the lines of the proof of Theorem 3, the instantaneous WEP $P_{e,\mathbf{D}}$ is upper bounded as

$$P_{e,\mathbf{D}} \le (M^{n_{min}} - 1) Q\left(\sqrt{\frac{SNR}{2n_t E_M}} d_{min}\right), \tag{33}$$

where $E_M = 2(M-1)/3$ and $d_{min} = \min_{\Delta\mathbf{x}, \Delta\mathbf{x} \ne \mathbf{O}_{n_{min} \times 1}} \|\mathbf{DP}\Delta\mathbf{x}\|$, with $\Delta\mathbf{x} \in \left\{\mathbf{x}\text{-}\mathbf{x}' | \mathbf{x}, \mathbf{x}' \in \mathcal{A}_{M-QAM}^{n_{min} \times 1}\right\}$ and $\mathbf{P}$ being the precoder with the ith and $n_{min} - i + 1^{th}$ subchannels paired using the proposed precoding scheme described in Section IV. So,

$$d_{min} = \min_i \left\{\rho_i \sqrt{\frac{2n_t \delta(\gamma_i, \mathcal{A}_{M-QAM})}{n_{min}}}\right\},$$

with $\delta(\gamma_i, \mathcal{A}_{M-QAM})$ given by (32). Observe that the scaling factor of $2n_t/n_{min}$ has been used to take into account the constraint that $\|\mathbf{P}\|^2 = n_t$. Since the values of $\delta(\gamma_i, \mathcal{A}_{M-QAM})$ are known, we can enhance the error performance of the precoder by pre-multiplying the precoding matrix with a power control matrix $\mathbf{\Upsilon} = \text{diag}(\tau_1, \tau_2, \cdots, \tau_{n_{min}/2}, \tau_{n_{min}/2}, \cdots, \tau_2, \tau_1)$ such that

$$\tau_i^2 \rho_i^2 \delta(\gamma_i, \mathcal{A}_{M-QAM}) = \eta^2, \quad \forall i \in \left\{1, 2, \cdots, \frac{n_{min}}{2}\right\}, \tag{34}$$

where η is a constant and the power constraint on $\mathbf{\Upsilon}$ is such that $\|\mathbf{\Upsilon}\|^2 = 2\sum_{i=1}^{n_{min}/2} \tau_i^2 = n_{min}$. Due to this power constraint, from (34), we obtain

$$\tau_i = \sqrt{\frac{n_{min}}{2\rho_i^2 \delta(\gamma_i, \mathcal{A}_{M-QAM})} \left(\sum_{j=1}^{n_{min}/2} \frac{1}{\rho_j^2 \delta(\gamma_j, \mathcal{A}_{M-QAM})}\right)^{-1}},$$

where $\delta(\gamma_i, \mathcal{A}_{M-QAM})$ is obtainable from (32). Hence, the proposed precoder has the structure given in (9), where

$$\mathbf{M}_i = \sqrt{\frac{2n_t \tau_i^2}{n_{min}}} \begin{bmatrix} \cos\psi_i \cos\theta_i & -\cos\psi_i \sin\theta_i \\ \sin\psi_i \sin\theta_i & \sin\psi_i \cos\theta_i \end{bmatrix},$$

with ψ_i and θ_i being the approximately optimal values obtainable from (21) and (22), respectively, both depending on γ_i and M. For example, for a 4×4 system using 4-QAM signalling, if, for some channel realization, $\gamma_1 = \tan^{-1}\left(\frac{\sigma_4}{\sigma_1}\right) = \frac{1}{4}$ and $\gamma_2 = \tan^{-1}\left(\frac{\sigma_3}{\sigma_2}\right) = \tan^{-1}\left(\sqrt{\frac{2}{3}}\right)$, then, from Table I, $\theta_1 = \tan^{-1}(1/2)$, $\psi_1 = 0$, $\theta_2 = \pi/4$, $\psi_2 = \tan^{-1}\left(\frac{1}{\sqrt{3}\tan(\gamma_2)}\right)$ and $\tau_1 = \sqrt{\frac{5\eta^2}{(\sigma_1^2 + \sigma_4^2)\cos^2\gamma_1}}$, $\tau_2 = \sqrt{\frac{(1+3\tan^2\gamma_2)\eta^2}{2(\sigma_2^2 + \sigma_3^2)\sin^2\gamma_2}}$, $\eta^2 = 2\left(\frac{5}{(\sigma_1^2 + \sigma_4^2)\cos^2\gamma_1} + \frac{1+3\tan^2\gamma_2}{2(\sigma_2^2 + \sigma_3^2)\sin^2\gamma_2}\right)^{-1}$.

The upper bound on the instantaneous WEP is now given as

$$P_{e,\mathbf{D}} \leq (M^{n_{min}} - 1) Q\left(\sqrt{\frac{SNR}{n_{min}E_M}}\eta\right), \tag{35}$$

where

$$\eta = \sqrt{\frac{n_{min}}{2}\left(\sum_{j=1}^{n_{min}/2} \frac{1}{\rho_j^2 \delta(\gamma_j, \mathcal{A}_{M-QAM})}\right)^{-1}}. \tag{36}$$

It can easily be checked that

$$Q\left(\sqrt{\frac{SNR}{2n_t E_M}}d_{min}\right) \geq Q\left(\sqrt{\frac{SNR}{n_{min}E_M}}\eta\right)$$

and hence, the upper bound in (35) is lower than that in (33). Therefore, the use of the power control matrix enhances error performance. Note that the symbols of each subsystem can be decoded independently from the symbols of the other subsystems. Hence, the ML-decoding complexity offered by our precoding scheme is $\mathcal{O}(\sqrt{M})$.

A similar approach of using a power control matrix has been taken in [14] for 4-QAM, but since we need to have explicit values of $\delta(\gamma_i, \mathcal{A}_{M-QAM})$, applying this scheme for the E-d_{min} precoder with larger constellations is not feasible. Structurally, the E-d_{min} precoder and the X-precoder differ from (9) in that for the E-d_{min} precoder, $\mathbf{M}_i$ is optimized using an additional parameter ϕ_i (as shown in (13)), while for the X-precoder, $\mathbf{M}_i$ is optimized with $\tau_i = 1$ and $\psi_i = \pi/4$. Table II gives a comparison of the various low ML-decoding complexity precoding schemes.

VI. DIVERSITY GAIN

The E-d_{min} precoder, the X-precoder and the Y-precoder have all been shown to guarantee a diversity gain equal to $\left(n_t - \frac{n_{min}}{2} + 1\right)\left(n_r - \frac{n_{min}}{2} + 1\right)$. Recall that the condition in Theorem 3 is only a sufficient condition for achieving full-diversity gain equal to $n_t n_r$. It is not necessary that $\mathbf{P}$ be such that $[\mathbf{P}\Delta\mathbf{x}]_1 \neq 0$, for $\Delta\mathbf{x} \in \{\mathbf{x}\text{-}\mathbf{x}', \ \mathbf{x},\mathbf{x}' \in \mathcal{A}^{n_{min}\times 1}\}$. This can be seen by noting that for $n_t = 2$ and 4-QAM, our precoder does not satisfy the condition when $\theta^* = \pi/4$, but still gives full-diversity. This is proved in the following lemma.

Lemma 2: The proposed precoder offers full-diversity, i.e., a diversity gain equal to $2n_r$ for $n_t = 2$.

Proof: Consider the precoder given by

$$\mathbf{P} = \begin{bmatrix} \cos\left(0.5\tan^{-1}2\right) & -\sin\left(0.5\tan^{-1}2\right) \\ \sin\left(0.5\tan^{-1}2\right) & \cos\left(0.5\tan^{-1}2\right) \end{bmatrix},$$

which is the full-diversity rotation matrix [22] in 2 dimensions and has the highest non-zero product distance among all 2×2 sized orthogonal matrices. This precoder, which we call the lattice precoder for $n_t = 2$, has full-diversity from Theorem 3. Clearly, $\delta(\gamma, \mathcal{A}_{M-QAM})$ for any value of γ is greater for our precoder than that for the lattice precoder, since our precoder is approximately optimal among real-valued precoders. So, our precoder has better error performance than the lattice precoder. Hence, our precoder too offers full-diversity, like the lattice precoder for $n_t = 2$. ∎

From Lemma 2, Theorem 2 and Theorem 3, one would be inclined to believe that for $n_t > 2$, a subsystem with index i, for which the ith and the $n_{min} - i + 1^{th}$ virtual subchannels are paired and the ith and the $n_{min} - i + 1^{th}$ symbols precoded by the scheme proposed in Section IV, has a diversity gain of $(n_t - i + 1)(n_r - i + 1)$, with $i = 1, 2, \cdots, n_{min}/2$, in which case the diversity gain of the whole system would be the minimum of the diversity gains of all the subsystems, i.e., $(n_t - n_{min}/2 + 1)(n_r - n_{min}/2 + 1)$. In fact, the diversity gains of systems using the E-d_{min} precoder and the X-precoder have been claimed to be $(n_t - n_{min}/2 + 1)(n_r - n_{min}/2 + 1)$ due to this reason. It must be noted that the power control matrix Υ plays an important role in the error performance of our precoder (also the E-d_{min} precoder for 4-QAM), as explained in Section V. Before we analyze the achievable diversity gain of the system with the proposed precoding scheme, the following important observation needs to be made about $\delta(\gamma_i, \mathcal{A}_{M-QAM})$. Since $\sigma_1 \geq \sigma_2 \geq \cdots \sigma_{n_{min}}$, we have $\frac{\sigma_{n_{min}}}{\sigma_1} \leq \frac{\sigma_{n_{min}-1}}{\sigma_2} \leq \cdots \frac{\sigma_{\frac{n_{min}}{2}+1}}{\sigma_{\frac{n_{min}}{2}}}$. Consequently,

$$\tan^{-1}\left(\frac{\sigma_{n_{min}}}{\sigma_1}\right) \leq \tan^{-1}\left(\frac{\sigma_{n_{min}-1}}{\sigma_2}\right) \leq \cdots \tan^{-1}\left(\frac{\sigma_{\frac{n_{min}}{2}+1}}{\sigma_{\frac{n_{min}}{2}}}\right)$$

and therefore, $\gamma_1 \leq \gamma_2 \cdots \leq \gamma_{n_{min}/2}$. From Fig. 1, except for the case of 4-QAM, we can conclude that $\delta(\gamma_i, \mathcal{A}_{M-QAM}) \leq \delta(\gamma_j, \mathcal{A}_{M-QAM})$, for $i < j$. Due to this fact, although it is expected that for $1 \leq i < j \leq n_{min}/2$, $\rho_i^2 \geq \rho_j^2$, it is not guaranteed that $\rho_i^2 \delta(\gamma_i, \mathcal{A}_{M-QAM}) > \rho_j^2 \delta(\gamma_j, \mathcal{A}_{M-QAM})$, due to which even without the use of Υ, the overall diversity gain of the system might be higher than $(n_t - n_{min}/2 + 1)(n_r - n_{min}/2 + 1)$ (this holds true even for the X-precoder). With the use of Υ for our proposed precoder, the channel dependent instantaneous WEP is dependent on η, as seen in (35). Let

$$\zeta \triangleq \frac{\eta}{\rho_1 \sqrt{\delta(\gamma_1, \mathcal{A}_{M-QAM})}}$$

and P_ζ be the probability that $\zeta < 1$.

In Table III, we tabulate the values of ζ_{min}, which is the minimum value of ζ obtained on simulations for 10^7 channel realizations, and P_ζ, which is again calculated by simulating 10^7 channel realizations, for different MIMO systems. In the table, we observe that for $n_t = 16, 32$ and for $M \geq 64$, ζ is always

greater that 1. This can be attributed to the fact that for higher values of n_{min}, the ratio of $\sigma_{n_{min}}$ to σ_1 is very low and the corresponding value of $\delta(\gamma_1, \mathcal{A}_{M-QAM})$ is also very low. For such systems, we can safely say that the full-diversity gain equal to $n_t n_r$ is achieved (since σ_1^2 is associated with a diversity gain of $n_t n_r$). For other systems, the simulations results in Table III seem to indicate that there exists a $\zeta_{min} > 0$ such that $\zeta_{min} \leq \zeta$, i.e., ζ is lower bounded by ζ_{min}. So, from (35),

$$P_{e,\mathbf{D}} \leq (M^{n_{min}} - 1) Q \left(\sqrt{\frac{SNR.\zeta_{min}^2 \rho_1^2 \delta(\gamma_1, \mathcal{A}_{M-QAM})}{n_{min} E_M}} \right).$$

Let $\delta_M = \min\{\delta(\gamma_1, \mathcal{A}_{M-QAM})\}$, which is a constant depending on M. Then,

$$
\begin{aligned}
P_{e,\mathbf{D}} &\leq (M^{n_{min}} - 1) Q \left(\sqrt{\frac{SNR.\zeta_{min}^2 \rho_1^2 \delta_M}{n_{min} E_M}} \right) \leq (M^{n_{min}} - 1) Q \left(\sqrt{\frac{SNR.\zeta_{min}^2 \sigma_1^2 \delta_M}{n_{min} E_M}} \right) \\
&= (M^{n_{min}} - 1) Q \left(\sqrt{\left(\frac{\zeta_{min}^2 \delta_M}{n_{min} E_M} \right) \lambda_1 SNR} \right),
\end{aligned}
$$

where, as used throughout the paper, $\lambda_1 = \sigma_1^2$. From Theorem 1, we obtain, as $SNR \to \infty$,

$$P_e \leq C.SNR^{-n_t n_r} + o\left(SNR^{-n_t n_r} \right).$$

where

$$C = (M^{n_{min}} - 1) \frac{a_1 (2n_t n_r - 1)(2n_t n_r - 3) \cdots 1}{2n_t n_r} \left(\frac{\delta_M \zeta_{min}^2}{n_{min} E_M} \right)^{-n_t n_r}, \tag{37}$$

with a_1 being a constant in the expression for the marginal PDF of λ_1, as defined in Theorem 2. Therefore, the overall diversity gain of the system is $n_t n_r$. Note that in (37), δ_M and ζ_{min} define the coding gain - the higher the value of ζ_{min} and δ_M, the better the error performance. It is not known if ζ_{min} can be obtained analytically. The values in Table III are only indicative of what the actual ζ_{min} is likely to be. For example, for the 16×16 system with 64-QAM, ζ_{min} is likely to be greater than 1. Thus, we have shown that our precoding scheme provides full-diversity. This claim is supported by the WEP plots for different MIMO systems, shown in the following section.

VII. SIMULATION RESULTS

For all simulations, we consider the Rayleigh fading channel with prefect CSIT and CSIR. We consider three MIMO systems - 2×2, 4×4 and 8×8 MIMO systems. For the 2×2 MIMO system, the rival precoders for our precoder are the E-d_{min} precoder and the X-precoder. We have left out the Y-precoder since it has been shown in [16] to have an error performance comparable with that of the X-precoder for

4-QAM, while for 16-QAM, it is not expected to beat the X-precoder, as can be inferred from Fig. 3. The constellations employed are 4-QAM and 16-QAM. For 16-QAM, the E-d_{min} precoder is not considered since it is very hard to obtain and not explicitly stated in literature. For the X-precoder, we have obtained the approximately optimal angles for 16-QAM using a numerical search for $\gamma = k.\Delta$, $k = 1, 2, \cdots, \lfloor \frac{\pi}{4\Delta} \rfloor$, $\Delta = 0.001$, and have used a look-up table to obtain the appropriate angle for the corresponding value of γ during simulations. A look-up table is necessary since the approximately optimal angle for the X-precoder is not a weighted sum of shifted step functions like that for our precoder. Fig. 5 shows the plots of the word error probability (WEP) as a function of the average SNR at each receive antenna for the 2×2 system. As expected, the E-d_{min} precoder has the best error performance for 4-QAM, marginally beating our precoder, which in turn significantly beats the X-precoder. For 16-QAM, our precoder beats the X-precoder by about 1.5dB at an SNR of 30dB.

For 4×4 and 8×8 systems, we also consider the Lattice precoder, which is the orthogonal matrix with the largest known non-zero product distance for $n_{min} = n_t$ real dimensions, and given explicitly in [22]. This precoder has been shown in Theorem 3 to offer full-diversity. The plots of the WEP for the 4×4 system and the 8×8 system are given in Fig. 6 and Fig. 7, respectively. The plots indicate that the E-d_{min} precoder and our proposed precoder offer full-diversity, since they beat the full-diversity achieving Lattice precoder (even the X-precoder appears to offer full-diversity, losing out in coding gain only. The explanation for this has already been given in Section VI). Our precoder significantly outperforms the X-precoder while having lower expected ML-decoding complexity (as shown in Theorem 4), while the E-d_{min} precoder has the best error performance for 4-QAM, marginally beating our precoder, but this is at the expense of ML-decoding complexity. In Table IV, by simulating 10^6 channel realizations, we have tabulated the probability that ML-decoding can be done without searching over any of the signal points for 4- and 16-QAM. It can be noted that for the 2×2 MIMO system with 4-QAM, for more than 50% of the channel realizations, no search over any of the signal points is required, while for the 4×4 and the 8×8 MIMO systems, half the number of subsystems do not require any search over the constellation points for more than 99% of the channel realizations. This advantage, however, diminishes with the increase in constellation size.

VIII. DISCUSSION

For systems with full CSIT, we have proposed a real-valued precoder for $n_t = 2$, which, for QAM constellations, is approximately optimal among all real-valued precoders based on the SVD of the channel matrix and has an expected ML-decoding complexity lower than $\mathcal{O}(\sqrt{M})$. The advantage of the proposed

precoder over the E-d_{min} precoder is that it is much easier to obtain for larger QAM constellations and it also has lower ML-decoding complexity, while the loss in error performance for 4-QAM is only marginal. The proposed precoder handsomely beats the X-precoder in error performance while having lower expected ML-decoding complexity. A precoding scheme for $n_t > 2$ is also given and this scheme is shown to offer full-diversity with QAM constellations. It would be interesting to design low ML-decoding complexity, full-rate, full-diversity precoders for more realistic scenarios, like for systems with imperfect CSIT or partial CSIT.

ACKNOWLEDGEMENTS

REFERENCES

[1] V. Tarokh, N. Seshadri and A. R Calderbank, "Space time codes for high date rate wireless communication : performance criterion and code construction," *IEEE Trans. Inf. Theory*, vol. 44, no. 2, pp. 744-765, Mar. 1998.

[2] B. A. Sethuraman, B. S. Rajan and V. Shashidhar, "Full-diversity, high-rate space-time block codes from division algebras," *IEEE Trans. Inf. Theory*, vol. 49, no. 10, pp. 2596-2616, Oct. 2003.

[3] F. Oggier, G. Rekaya, J. C. Belfiore and E. Viterbo, "Perfect space time block codes," *IEEE Trans. Inf. Theory,* vol. 52, no. 9, pp. 3885-3902, Sep. 2006.

[4] T. M. Cover and J. A. Thomas, "Elements of information theory," John Wiley and Sons, 2nd Ed., Jul. 2006.

[5] T. K. Lo, "Maximum ratio transmission," *IEEE Trans. Commun.*, vol. 47, no. 10, pp. 1458-1461, Oct. 1999.

[6] P. Stoica and G. Ganesan, "Maximum-SNR spatial-temporal formatting designs for MIMO channels," *IEEE Trans. Signal Process.*, vol. 50, no. 12, pp. 3036-3042, Dec. 2002.

[7] H. Sampath, P. Stoica, and A. Paulraj, "Generalized linear precoder and decoder design for MIMO channels using the weighted MMSE criterion," *IEEE Trans. Commun.*, vol. 49, no. 12, pp. 2198-2206, Dec. 2001.

[8] A. Scaglione, P. Stoica, S. Barbarossa, G. B. Giannakis and H. Sampath, "Optimal Designs for Space-Time Linear Precoders and Decoders," *IEEE Trans. Signal Process.*, vol. 50, no. 5, pp. 1051-1064, May 2002.

[9] P. Rostaing, O. Berder, G. Burel, and L. Collin, "Minimum BER diagonal precoder for MIMO digital transmission," *Signal Process.*, vol. 82, no. 10, pp. 1477-1480, Oct. 2002.

[10] D. P. Palomar, J.M. Cioffi and M.A. Lagunas, "Joint Tx-Rx Beamforming Design for Multicarrier MIMO Channels: A unified Framework for Convex Optimization," *IEEE. Trans. Signal Process.*, vol. 51, no. 9, pp. 2381-2401, Sep. 2003.

[11] C. Windpassinger and R. F. H. Fischer, "Low-Complexity Near-Maximum-Likelihood Detection and Precoding for MIMO Systems using Lattice Reduction," in the Proc. of the *Inf. Theory Workshop (ITW 03)*, Paris, France, Mar. 31 - Apr. 04, 2003.

[12] D. J. Love and R. W. Heath, Jr., "Multimode Precoding for MIMO Wireless Systems," *IEEE Trans. Signal Process.*, vol. 53, no. 10, Oct. 2005.

[13] G. Raleigh and J. Cioffi, "Spatio-Temporal Coding for Wireless Communication," *IEEE Trans. Commun.*, vol. 46, no. 3, pp. 357-366, Mar. 1998.

[14] B. Vrigneau, J. Letessier, P. Rostaing, L. Collin, and G. Burel, "Extension of the MIMO Precoder Based on the Minimum Euclidean Distance: A Cross-Form Matrix," *IEEE Journal Sel. Topics Signal Process.*, vol. 2, no. 2, pp. 135-146, Apr. 2008.

[15] L. Collin, O. Berder, P. Rostaing and G. Burel, "Optimal Minimum Distance Based Precoder for MIMO Spatial Multiplexing Systems," *IEEE Trans. Signal Process.*, vol. 52, no. 3, pp. 617-627, Mar. 2004.

[16] S. K. Mohammed, E. Viterbo, Y. Hong and A. Chockalingam, "MIMO Precoding with X- and Y-Codes," accepted for publication in the *IEEE Trans. Inf. Theory*, available online at arXiv, ID: arXiv:0912.1909.

[17] E. Viterbo and J. Boutros, "Universal lattice code decoder for fading channels," *IEEE Trans. Inf. Theory.*, vol. 45, no. 5, pp. 1639-1642, Jul. 1999.

[18] B. Hassibi and H. Vikalo, "On the sphere-decoding algorithm I. Expected complexity," *IEEE Trans. Signal Process.*, vol. 53, no. 8, Aug. 2005.

[19] Z. Wang and G. B. Giannakis, "A Simple and General Parameterization Quantifying Performance in Fading Channels," *IEEE Trans. Commun.*, vol. 51, no. 8, pp. 1389-1398, Aug. 2003.

[20] L. G. Ordonez, D. P. Palomar, A. P. Zamora and J. R. Fonollosa, "High-SNR analytical performance of Spatial Multiplexing MIMO Systems With CSI," *IEEE Trans. Signal Process.*, vol. 55, no. 11, pp. 5447-5463, Nov. 2007.

[21] H. J. Park, B. Li and E. Ayanoglu, "Multiple Beamforming with Constellation Precoding: Diversity Analysis and Sphere Decoding," in the Proc. of *Inf. Theory and Applications (ITA 2010)*, pp. 1-11, San Diego, USA, Jan. 31 - Feb. 05, 2010.

[22] *Full diversity rotations*, http://www1.tlc.polito.it/~viterbo/rotations/rotations.html.

M	γ	θ^*	$\tan\gamma\tan\psi^*$	(p,q)
4	$0 - \tan^{-1}\left(\frac{1}{\sqrt{7}}\right)$	$\tan^{-1}\left(\frac{1}{2}\right)$	0	$(0,1),\ (1,1)$
	$\tan^{-1}\left(\frac{1}{\sqrt{7}}\right) - \frac{\pi}{4}$	$\frac{\pi}{4}$	$\frac{1}{\sqrt{3}}$	$(0,1),\ (1,1),\ (1,0)$
16	$0 - 0.1018$	$\tan^{-1}\left(\frac{1}{4}\right)$	0	$(0,1),\ (1,3)$
	$0.1018 - 0.1567$	0.3474	0.1096	$(0,1),\ (1,3),\ (1,2)$
	$0.1567 - 0.3479$	0.4914	0.2277	$(0,1),\ (1,1),\ (1,2)$
	$0.3479 - \frac{\pi}{4}$	$\frac{\pi}{4}$	$\frac{1}{\sqrt{3}}$	$(0,1),\ (1,1),\ (1,0)$
64	$0 - 0.0273$	$\tan^{-1}\left(\frac{1}{8}\right)$	0	$(0,1),\ (1,7)$
	$0.0273 - 0.0354$	0.5450	0.0335	$(1,2),\ (2,3),\ (3,5)$
	$0.0354 - 0.0415$	0.3766	0.0393	$(1,2),\ (1,3),\ (2,5)$
	$0.0415 - 0.0519$	0.6325	0.0433	$(1,1),\ (2,3),\ (3,4)$
	$0.0519 - 0.0735$	0.2640	0.0620	$(0,1),\ (1,3),\ (1,4)$
	$0.0735 - 0.0975$	0.5763	0.0872	$(1,1),\ (1,2),\ (2,3)$
	$0.0975 - 0.1567$	0.3474	0.1096	$(0,1),\ (1,3),\ (1,2)$
	$0.1567 - \frac{\pi}{4}$	same as 16-QAM	same as 16-QAM	same as 16-QAM
256	$0 - 0.0071$	$\tan^{-1}\left(\frac{1}{16}\right)$	0	$(0,1),\ (1,15)$
	$0.0071 - 0.0139$	0.5103	0.0098	$(1,2),\ (4,7),\ (5,9)$
	$0.0139 - 0.0278$	0.1501	0.0197	$(0,1),\ (1,6),\ (1,7)$
	$0.0278 - 0.0494$	0.2114	0.0394	$(0,1),\ (1,4),\ (1,5)$
	$0.0494 - 0.0735$	0.2640	0.0620	$(0,1),\ (1,3),\ (1,4)$
	$0.0735 - \frac{\pi}{4}$	same as 64-QAM	same as 64-QAM	same as 64-QAM
1024	$0 - 0.0018$	$\tan^{-1}\left(\frac{1}{32}\right)$	0	$(0,1),\ (1,31)$
	$0.0018 - 0.0027$	0.1301	0.0022	$(1,8),\ (2,15),\ (3,23)$
	$0.0027 - 0.0042$	0.2300	0.0035	$(1,4),\ (3,13),\ (4,17)$
	$0.0042 - 0.0065$	0.7304	0.0053	$(1,1),\ (8,9),\ (9,10)$
	$0.0065 - 0.0086$	0.3509	0.0079	$(1,3),\ (3,8),\ (4,11)$
	$0.0086 - \frac{\pi}{4}$	same as 256-QAM	same as 256-QAM	same as 256-QAM

TABLE I

APPROXIMATELY OPTIMAL VALUES OF θ AND ψ FOR VARIOUS QAM CONSTELLATIONS

Precoder	ML-decoding complexity[‡] for $|\mathcal{A}| = M$	Existence for $|\mathcal{A}| = M$	Error performance
E-d_{min} precoder	$\mathcal{O}\left(M\sqrt{M}\right)$	exists only for 4-QAM	the best for $M = 4$ among known precoders
X-precoder	$\mathcal{O}\left(\sqrt{M}\right)$	not possible without the use of a look-up[¥] table for $M > 4$	worse than the E-d_{min} precoder and the proposed precoder
Y-precoder	$\mathcal{O}(1)$	closed form expression exists for any M, with $\mathcal{A}$ a 2-dimensional constellation [16]	better than X-precoders for ill-conditioned channels only
The proposed precoder	$\mathcal{O}\left(\sqrt{M}\right)$	easy to obtain for any M-QAM	much better than X-,Y-precoders

[‡] when $\gamma'_1 \leq \gamma \leq \gamma'_2$, for the E-$d_{min}$ precoder, a full search over all the signal points is needed, while for the proposed precoder, no search over signal points is needed.

[¥] amounts to storing the near-optimal angle values for $\gamma = k\Delta$, $k = 1, 2, \cdots, \lfloor\frac{\pi}{4\Delta}\rfloor$, where Δ is a suitable step size.

TABLE II

COMPARISON OF LOW ML-DECODING COMPLEXITY PRECODING SCHEMES

MIMO system	$M = 4$		$M = 16$		$M = 64$		$M = 256$		$M = 1024$	
	ζ_{min}	P_ζ	ζ_{min}	P_ζ	ζ_{min}	P_ζ	ζ_{min}	P_ζ	ζ_{min}	P_ζ
4×4	0.11	0.79	0.33	0.10	0.45	0.09	0.40	0.09	0.45	0.09
8×8	0.28	0.99	0.59	0.01	0.76	10^{-3}	0.77	1.1×10^{-3}	0.75	10^{-3}
16×16	0.35	1	0.72	9.1×10^{-4}	1.16	0	1.17	0	1.12	0
32×32	0.41	1	0.84	4×10^{-3}	1.87	0	1.75	0	1.9	0

TABLE III

CHARACTERISTICS OF ζ FOR DIFFERENT MIMO SYSTEMS

MIMO system		$M = 4$	$M = 16$
2×2	$Pr\{\frac{\sigma_2}{\sigma_1} \le \tan \gamma_2'\}$ [†]	0.5780	0.0612
4×4	$Pr\{\frac{\sigma_4}{\sigma_1} \le \tan \gamma_2'\}$	0.9942	0.3286
	$Pr\{\frac{\sigma_3}{\sigma_2} \le \tan \gamma_2'\}$	0.0620	8×10^{-6}
8×8	$Pr\{\frac{\sigma_8}{\sigma_1} \le \tan \gamma_2'\}$	1	0.8582
	$Pr\{\frac{\sigma_7}{\sigma_2} \le \tan \gamma_2'\}$	0.9969	0.0112
	$Pr\{\frac{\sigma_6}{\sigma_3} \le \tan \gamma_2'\}$	0.2179	0
	$Pr\{\frac{\sigma_5}{\sigma_4} \le \tan \gamma_2'\}$	4×10^{-6}	0

[†] $\gamma_2' = \tan^{-1}\left(\frac{1}{\sqrt{7}}\right)$ for $M = 4$ and $\gamma_2' \approx 0.1018$ for $M = 16$.

TABLE IV

PROBABILITY THAT NO SEARCH IS REQUIRED FOR EACH SUBSYSTEM OF DIFFERENT MIMO SYSTEMS
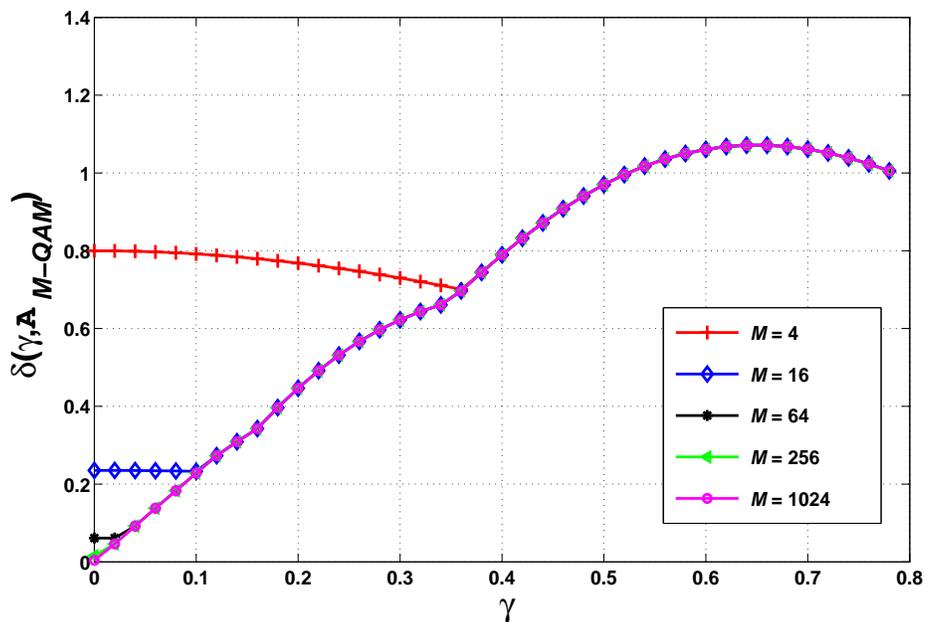
Fig. 1. $\delta(\gamma, \mathcal{A}_{M-QAM})$ as a function of γ for the proposed precoder for various QAM constellations
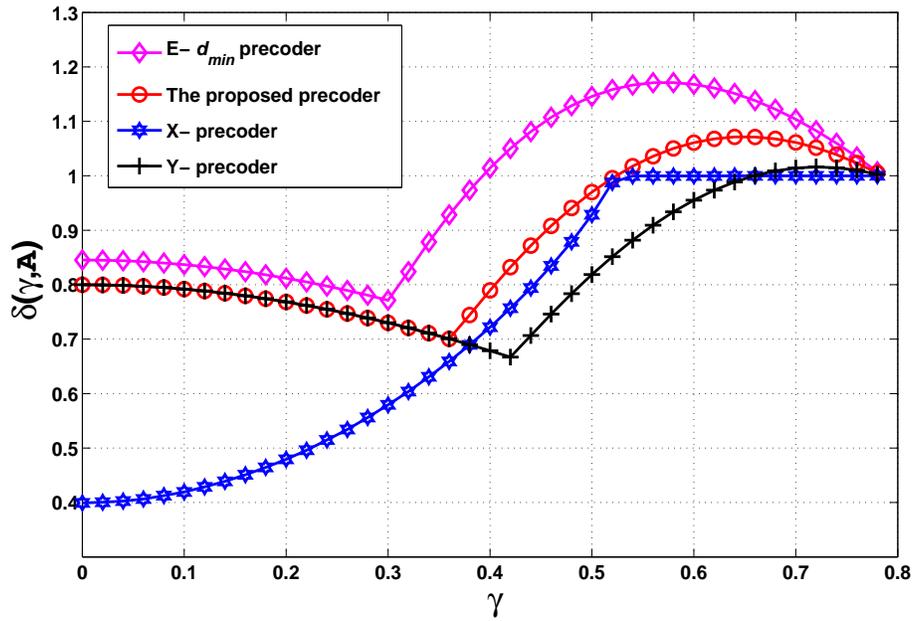
Fig. 2. $\delta(\gamma, \mathcal{A})$ comparison for $|\mathcal{A}| = 4$
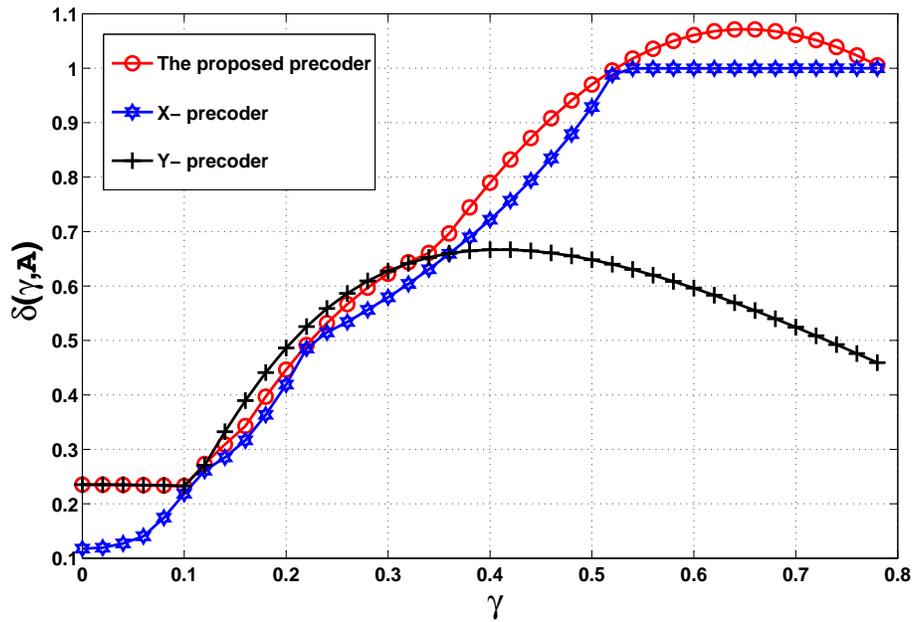
Fig. 3. $\delta(\gamma, \mathcal{A})$ comparison for $|\mathcal{A}| = 16$
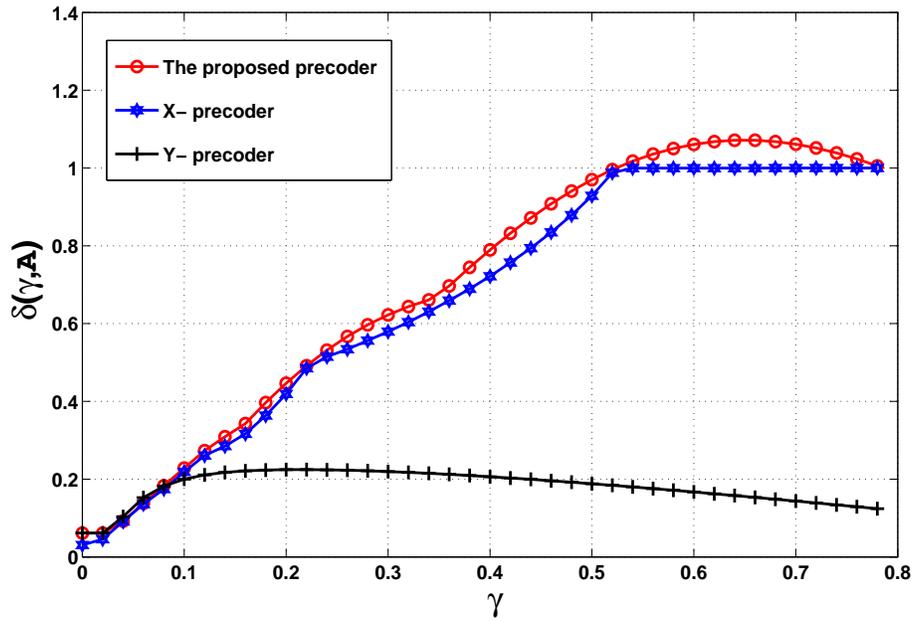
Fig. 4. $\delta(\gamma, \mathcal{A})$ comparison for $|\mathcal{A}| = 64$
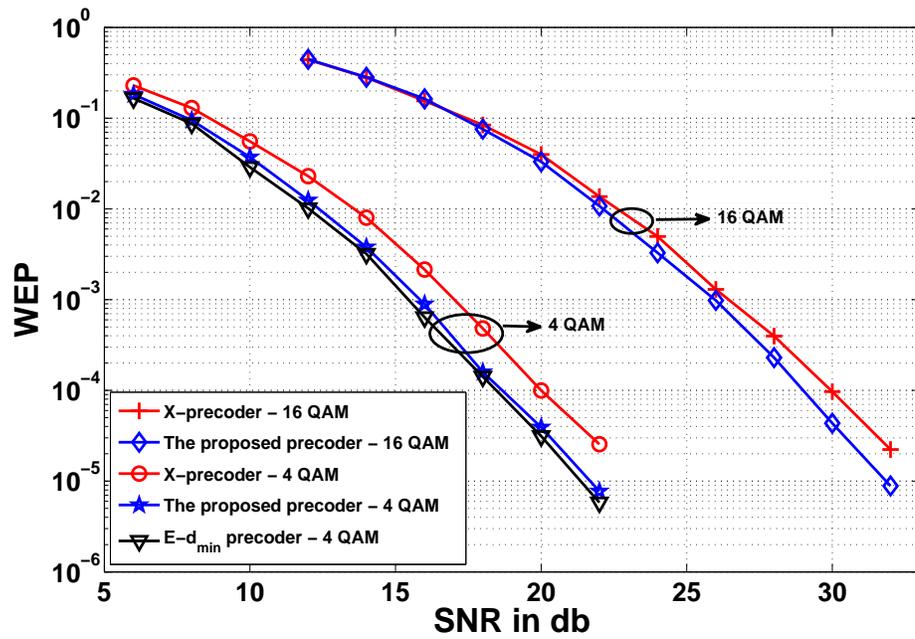
Fig. 5. WEP comparison for 2×2 MIMO systems for 4-QAM and 16-QAM
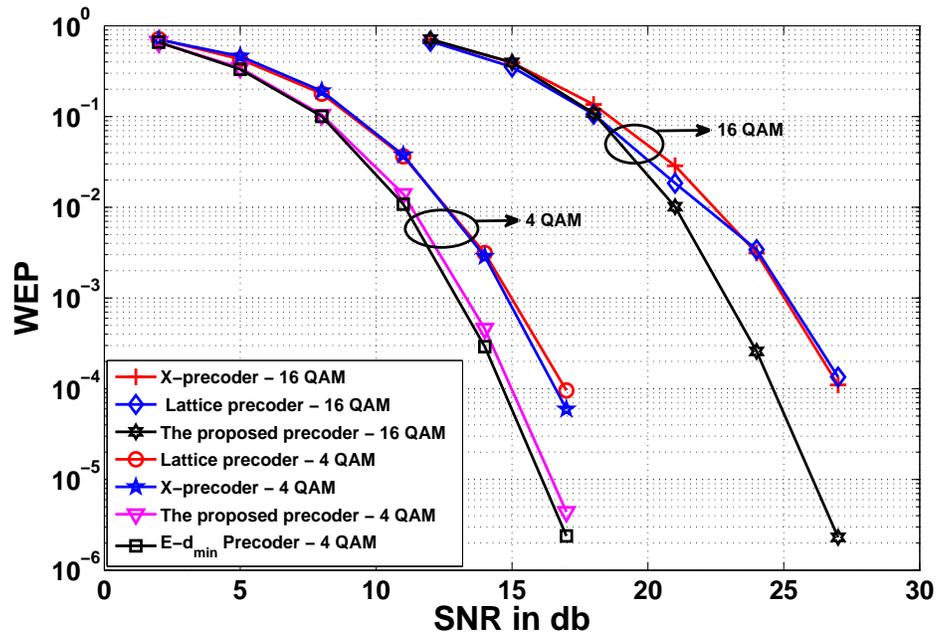
Fig. 6. WEP comparison for 4×4 MIMO systems for 4-QAM and 16-QAM
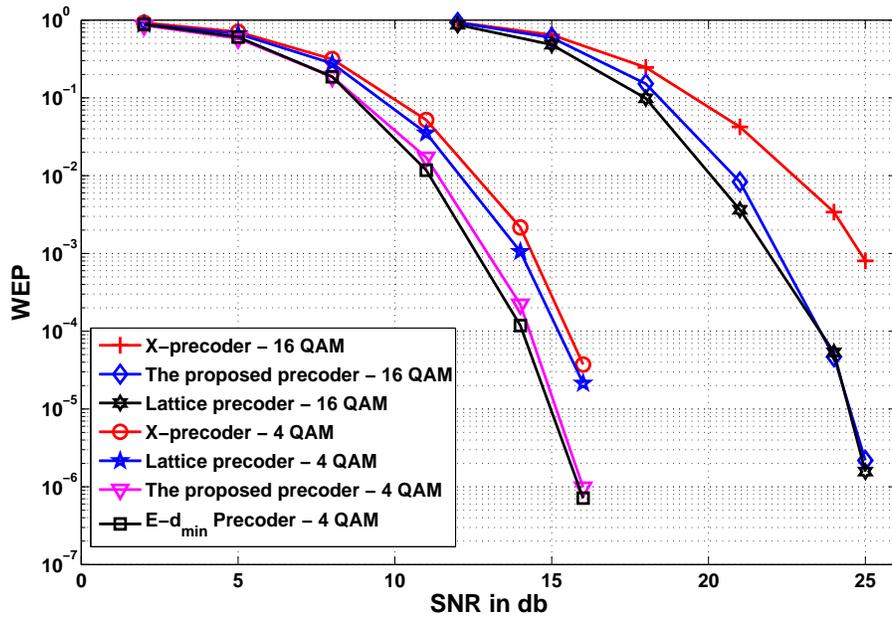
Fig. 7. WEP comparison for 8×8 MIMO systems for 4-QAM and 16-QAM